Evolução química em Galáxias

aulas 22 e 29/maio

Pagel, “Nucleosynthesis and Chemical Evolution of Galaxies”, 2009

Contexto

- Trata de reconstruir a história da composição química do gás em galáxias, através dos processos de formação de galáxias, formação estelar, evolução estelar, nuclossíntese e possivelmente trocas de material com o meio intergaláctico (gas flows)

- Desenvolveu-se a partir de estudos do Universo local

- Foi inicialmente explorado por Beatrice Tinsley: "Evolution of the Stars and Gas in Galaxies", Fundamentals of Cosmic Physics, 1980, vol 5, pp 287 - 388

- É uma peça chave hoje em dia no campo de Arqueologia Galáctica

Lookback time vs galactic archeology

Galaxies over lookback time

redshift

z=0 z=1 z=3 z=10

Hubble XDF

M31, apod

t=13.7E9 ~2E9 ~500E8

idade do universo (ano)

Archeology

Figure 9: (a) View of the courtyard today and (b) how it may have appeared in 30BC.

Credit: *High Fidelity Reconstruction of the Ancient Egyptian Temple of Kalabsha, Sundstedt*, Chalmers & Martinez (2004)

Our archeological site:
Chemical signatures in galaxy spectra

Signatures in a spectra

Credit: A. Kinney

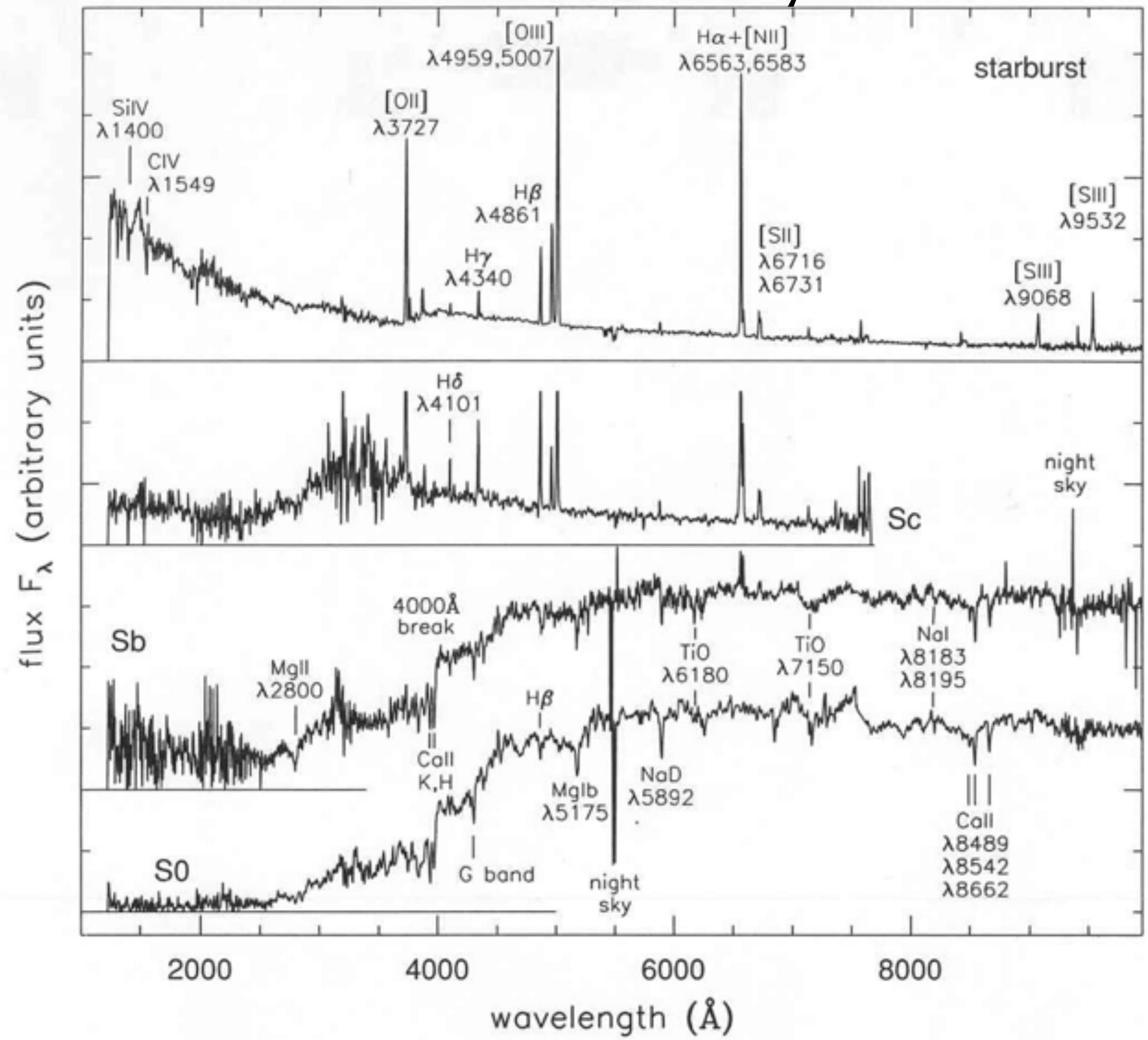

Absorption stellar spectra

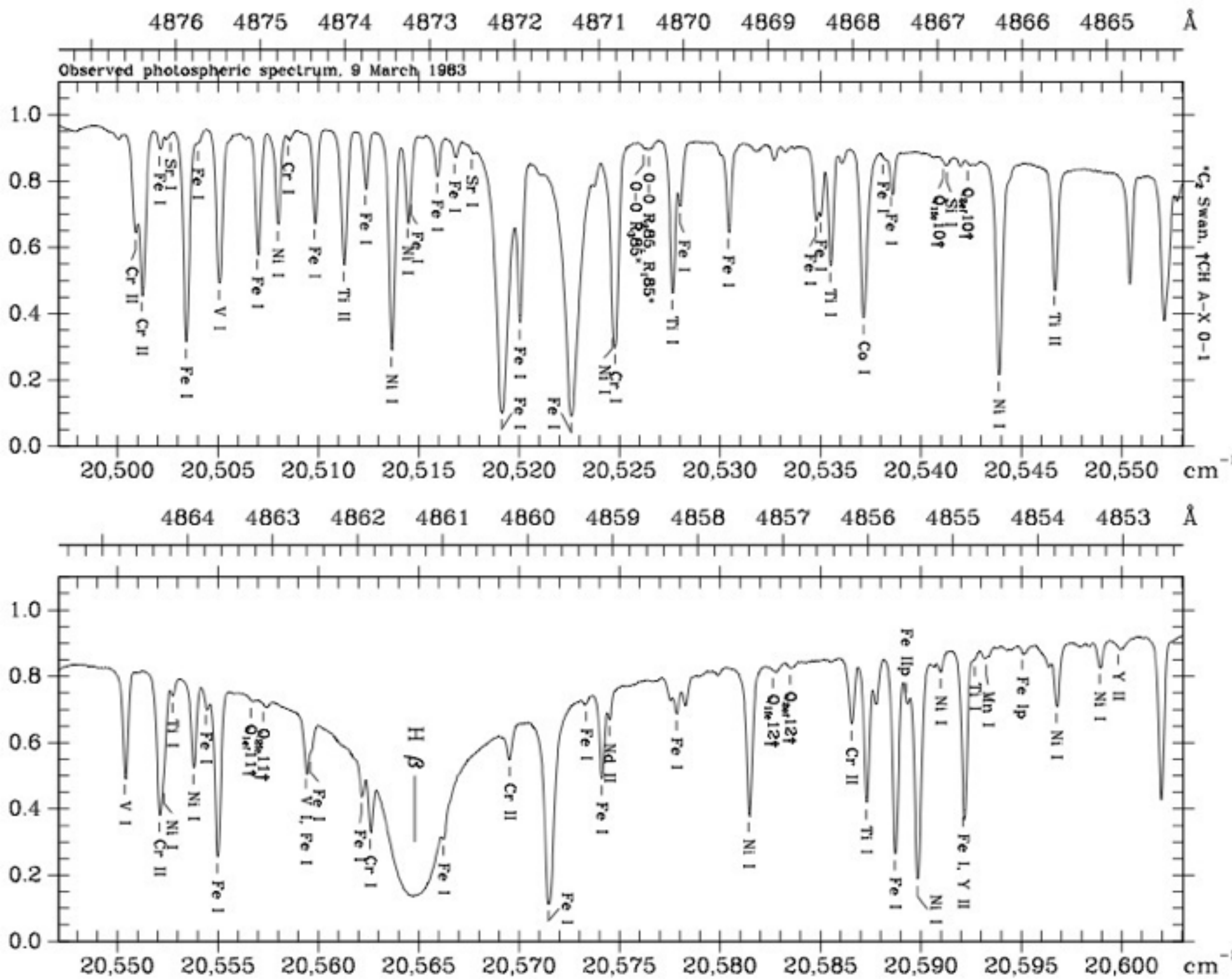

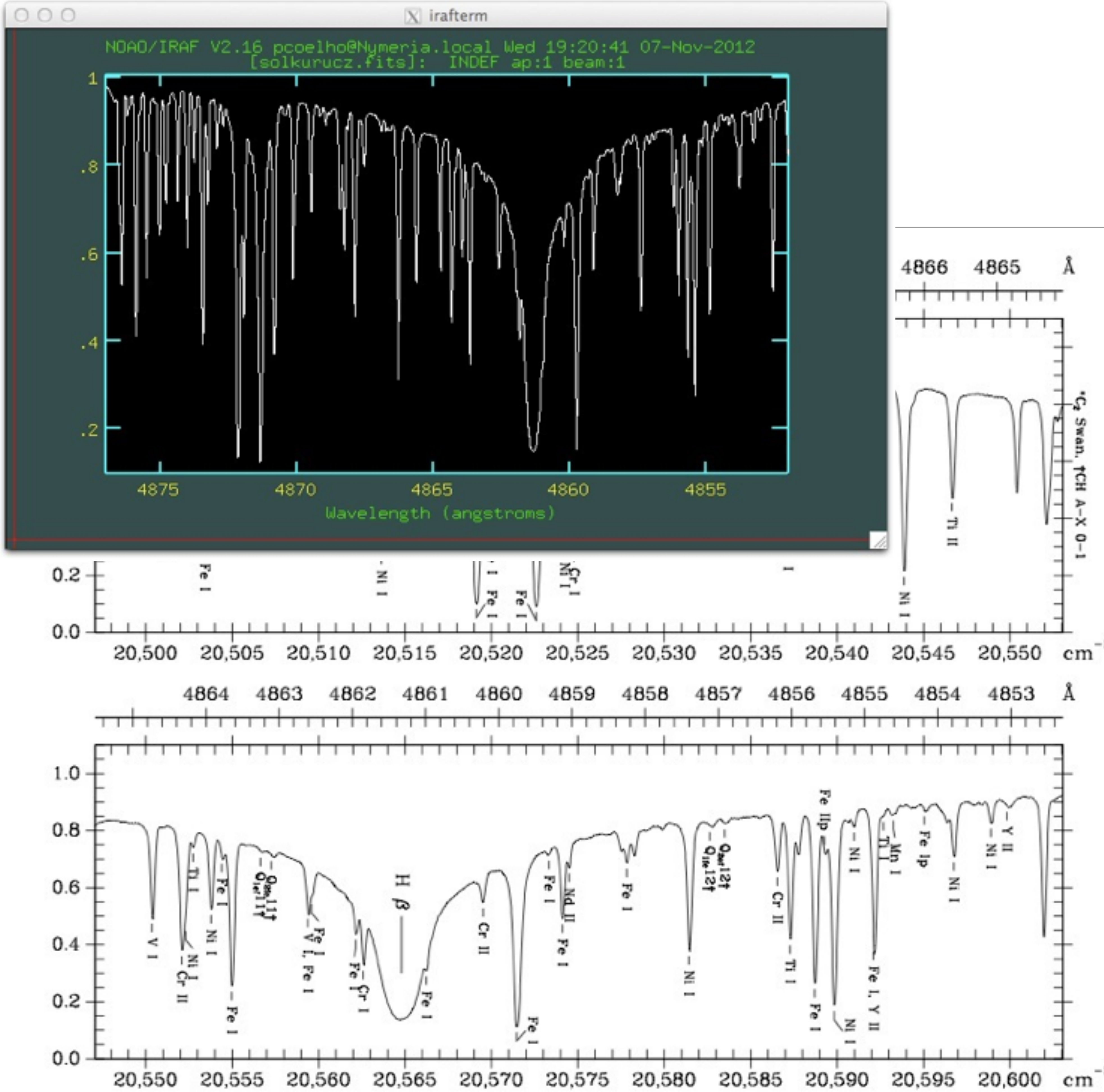
irafterm
NOAO/IRAF V2.16 pcoelho@Nymeria.local Wed 19:20:41 07-Nov-2012
[solkurucz.fits]: INDEF ap:1 beam:1
1
.8
.6
.4
.2
4875
4870
4865
4860
4855
Wavelength (angstroms)
4866
4865
Å
Fe I
Ni I
Fe I
Fe I
Ni I
Cr I
Ni I
Ti II
*C2 Swan, †CH A-X 0-1
0.2
0.0
20,500
20,505
20,510
20,515
20,520
20,525
20,530
20,535
20,540
20,545
20,550
cm⁻¹
4864
4863
4862
4861
4860
4859
4858
4857
4856
4855
4854
4853
Å
1.0
0.8
0.6
0.4
0.2
0.0
H β
V I
Cr II
Ni I
Ti I
Ni I
Fe I
Fe I
Q3H11†
Q1H11†
V I, Fe I
Fe I
Fe I
Cr I
Fe I
Cr II
Fe I
Fe I
Nd II
Fe I
Fe I
Ni I
Q2H12†
Q1H12†
Cr II
Ti I
Fe I
Fe IIp
Ni I
Fe I, Y II
Ni I
Ti I
Mn I
Fe Ip
Ni I
Ni I
Y II
20,550
20,555
20,560
20,565
20,570
20,575
20,580
20,585
20,590
20,595
20,600
cm⁻¹

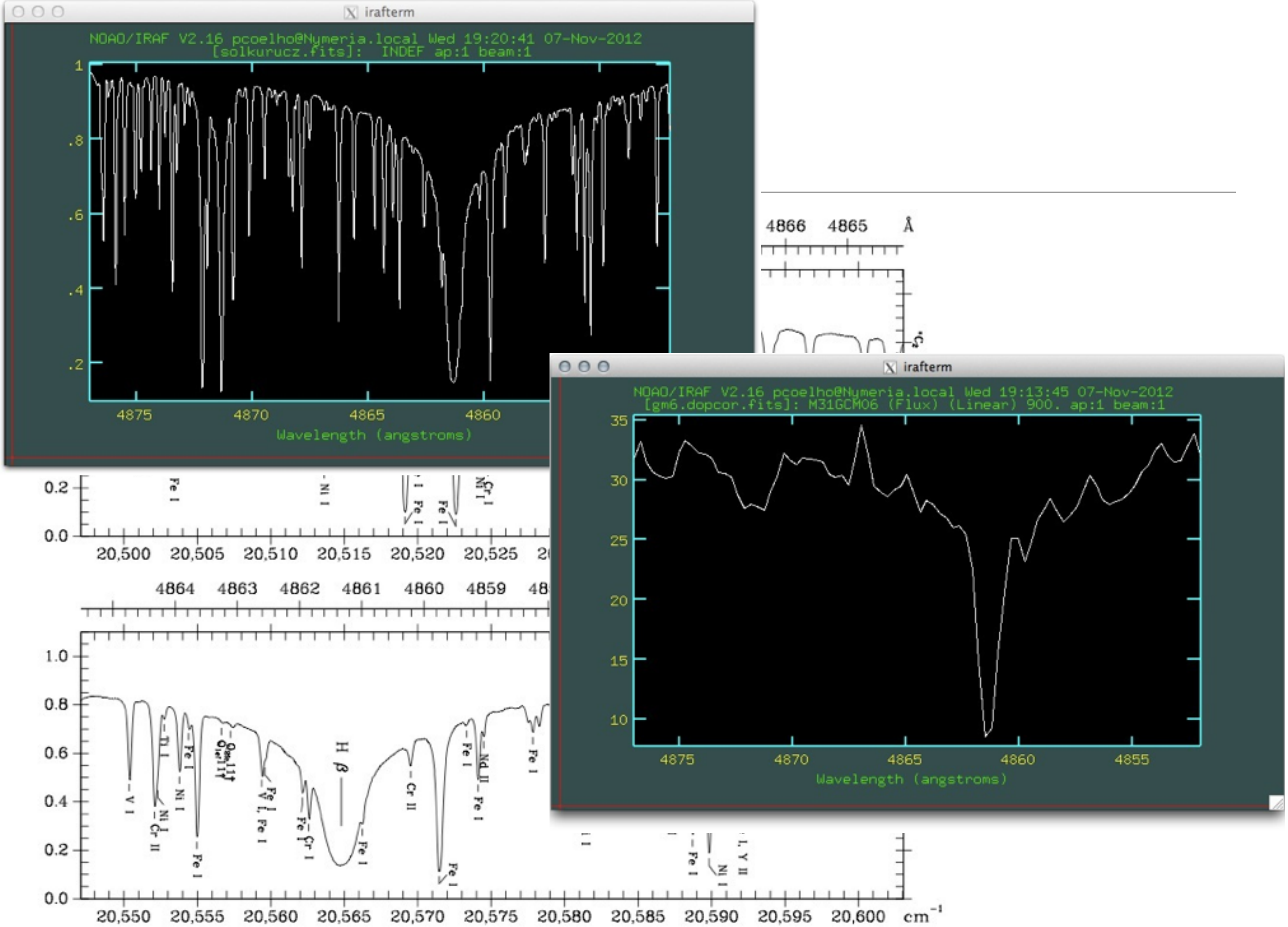

irafterm
NOAO/IRAF V2.16 pcoelho@Nymeria.local Wed 19:20:41 07-Nov-2012
[solkurucz.fits]: INDEF ap:1 beam:1
Wavelength (angstroms)
irafterm
NOAO/IRAF V2.16 pcoelho@Nymeria.local Wed 19:13:45 07-Nov-2012
[gm6.dopcor.fits]: M31GCM06 (Flux) (Linear) 900. ap:1 beam:1
Wavelength (angstroms)
H β
cm⁻¹
Å

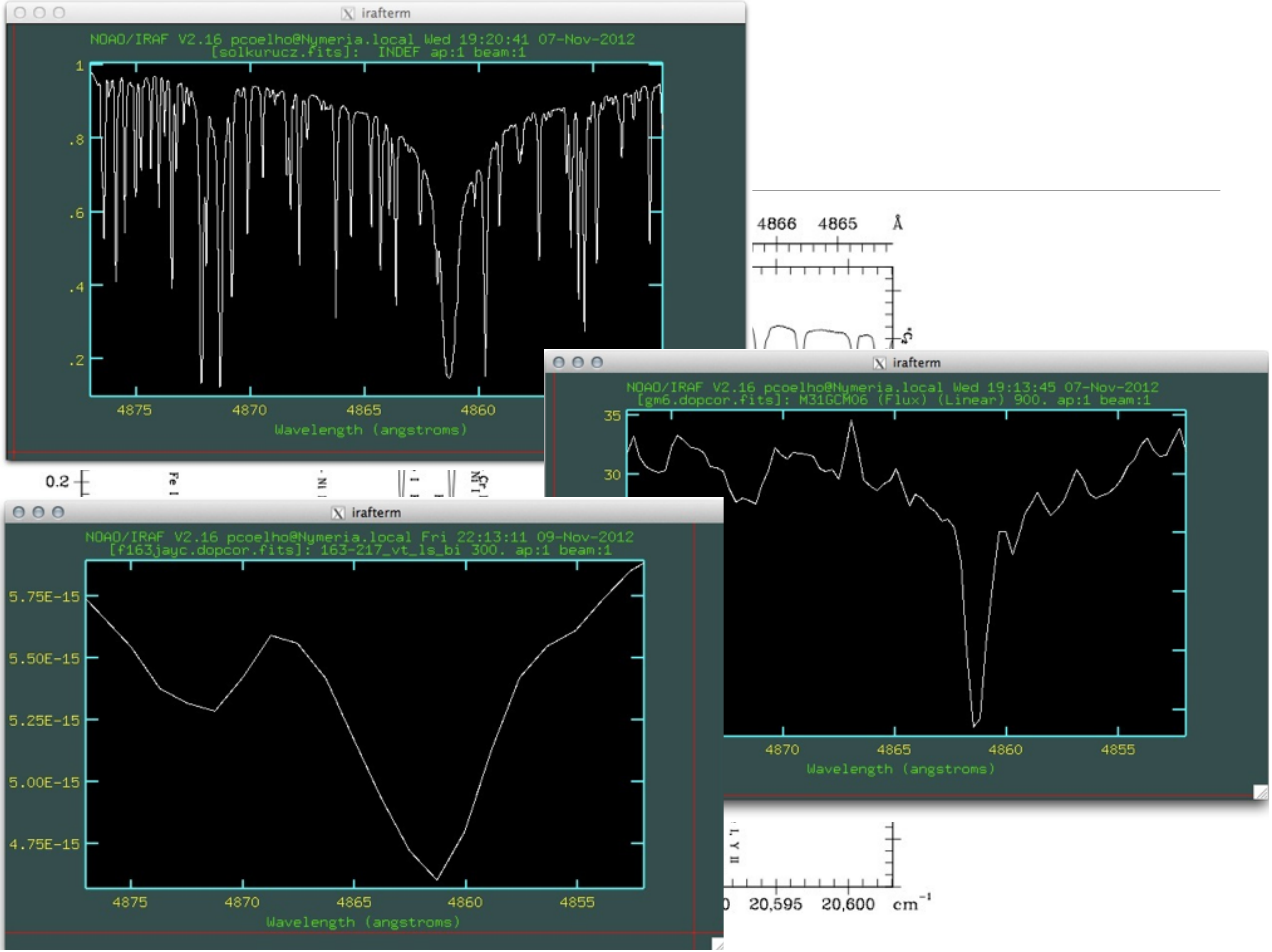

irafterm
NOAO/IRAF V2.16 pcoelho@Nymeria.local Wed 19:20:41 07-Nov-2012
[solkurucz.fits]: INDEF ap:1 beam:1
1
.8
.6
.4
.2
4875
4870
4865
4860
Wavelength (angstroms)
4866
4865
Å
0.2
Fe I
irafterm
NOAO/IRAF V2.16 pcoelho@Nymeria.local Wed 19:13:45 07-Nov-2012
[gm6.dopcor.fits]: M31GCM06 (Flux) (Linear) 900. ap:1 beam:1
35
30
4870
4865
4860
4855
Wavelength (angstroms)
irafterm
NOAO/IRAF V2.16 pcoelho@Nymeria.local Fri 22:13:11 09-Nov-2012
[f163jayc.dopcor.fits]: 163-217_vt_ls_bi 300. ap:1 beam:1
5.75E-15
5.50E-15
5.25E-15
5.00E-15
4.75E-15
4875
4870
4865
4860
4855
Wavelength (angstroms)
20,595
20,600
cm⁻¹

Supernovae and chemical evolution

Molecular clouds give birth to stars, which chemically enrich other clouds, which give birth to...

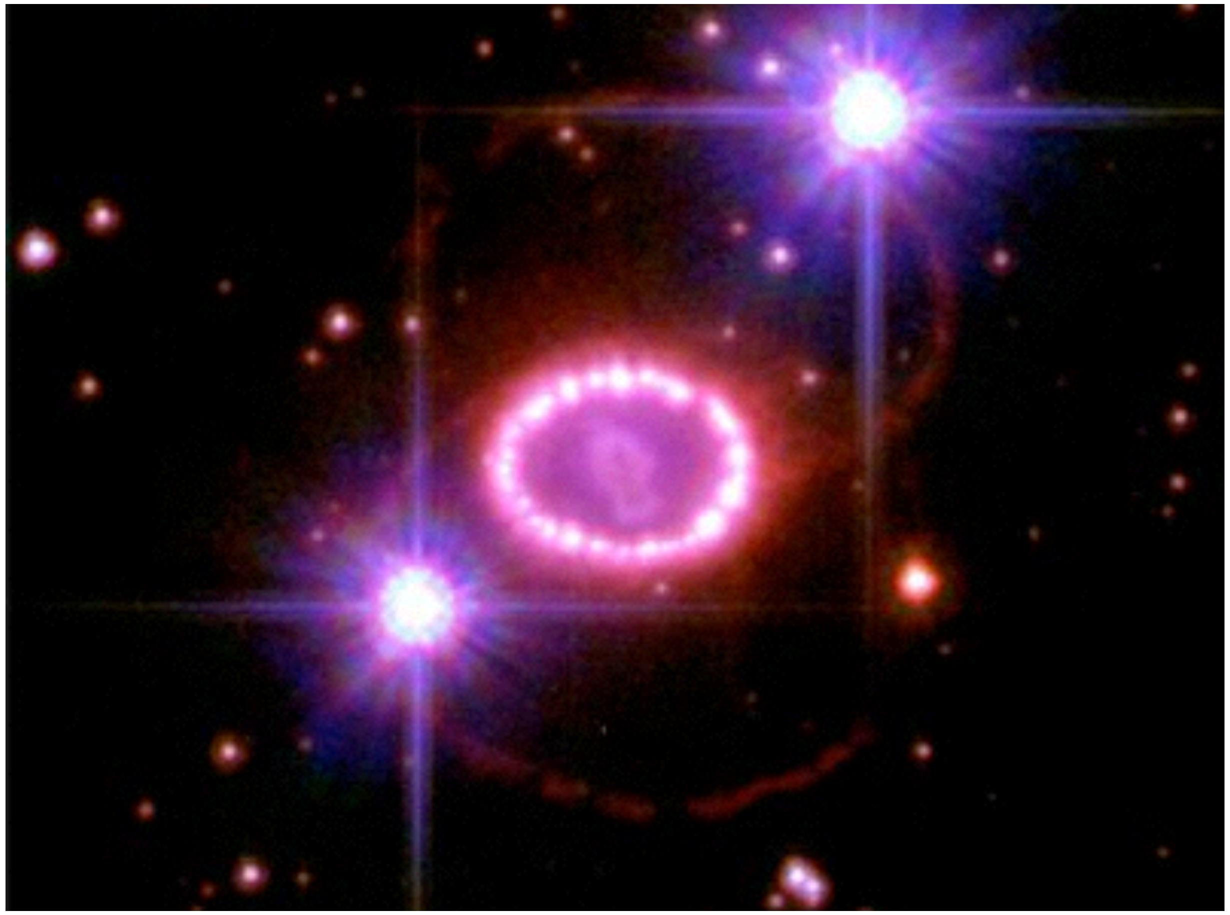

SN II, Ib and Ic: Core-collapse supernova
Progenitors: massive stars
Contribute with α (Ne, Mg, O, Si, S, Ar, Ca, Ti) and iron peak elements (V, Cr, Mn, Fe, Co, Ni)

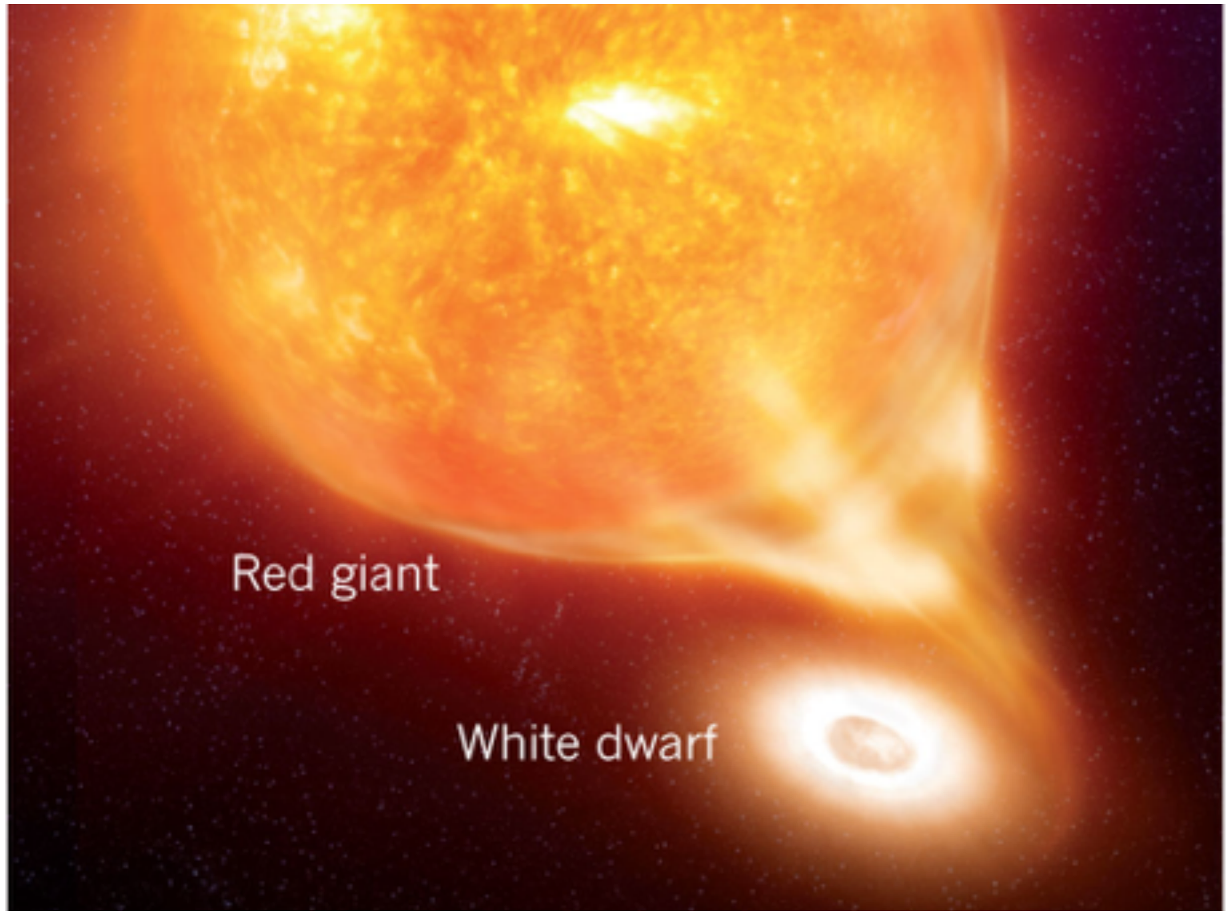

SN Ia
Explosion of white-dwarfs accreting matter
Progenitors: intermediate-mass stars
Contribute with Fe-peak elements ONLY

α-enhancement [α/Fe] in 2 slides

α/Fe as cosmic clock

- stars with high values of [α/Fe] were formed early in the evolution of a galaxy, when the contribution to the ISM from massive stars was still important
- galaxies with high values of [α/Fe] are systems where the bulk of the stars were formed early: is a measure of how extended was its star-formation

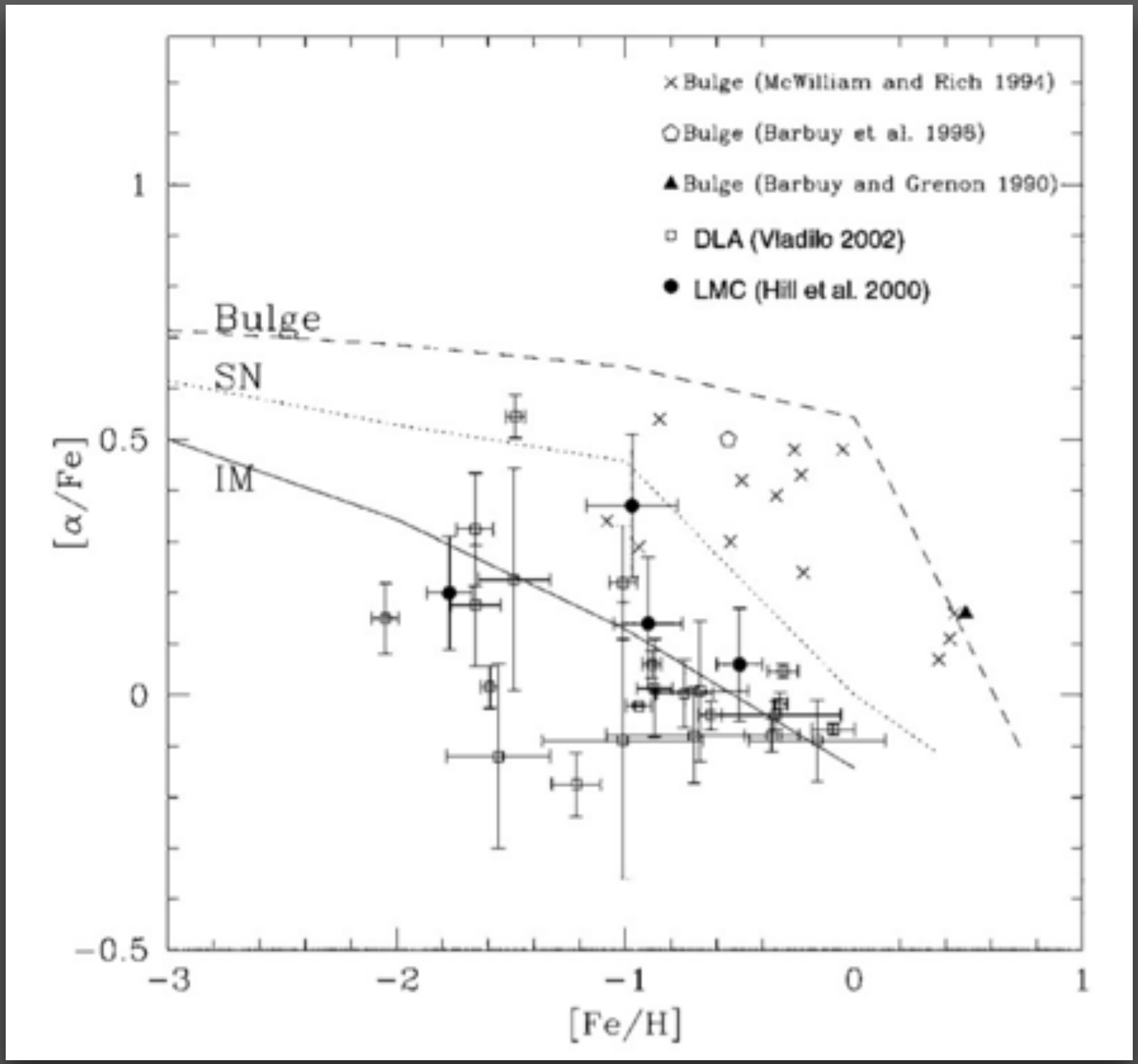

The predicted [α/Fe] ratios for three different histories of star formation but equal IMF and nucleosynthesis. Credit: Matteucci '03.

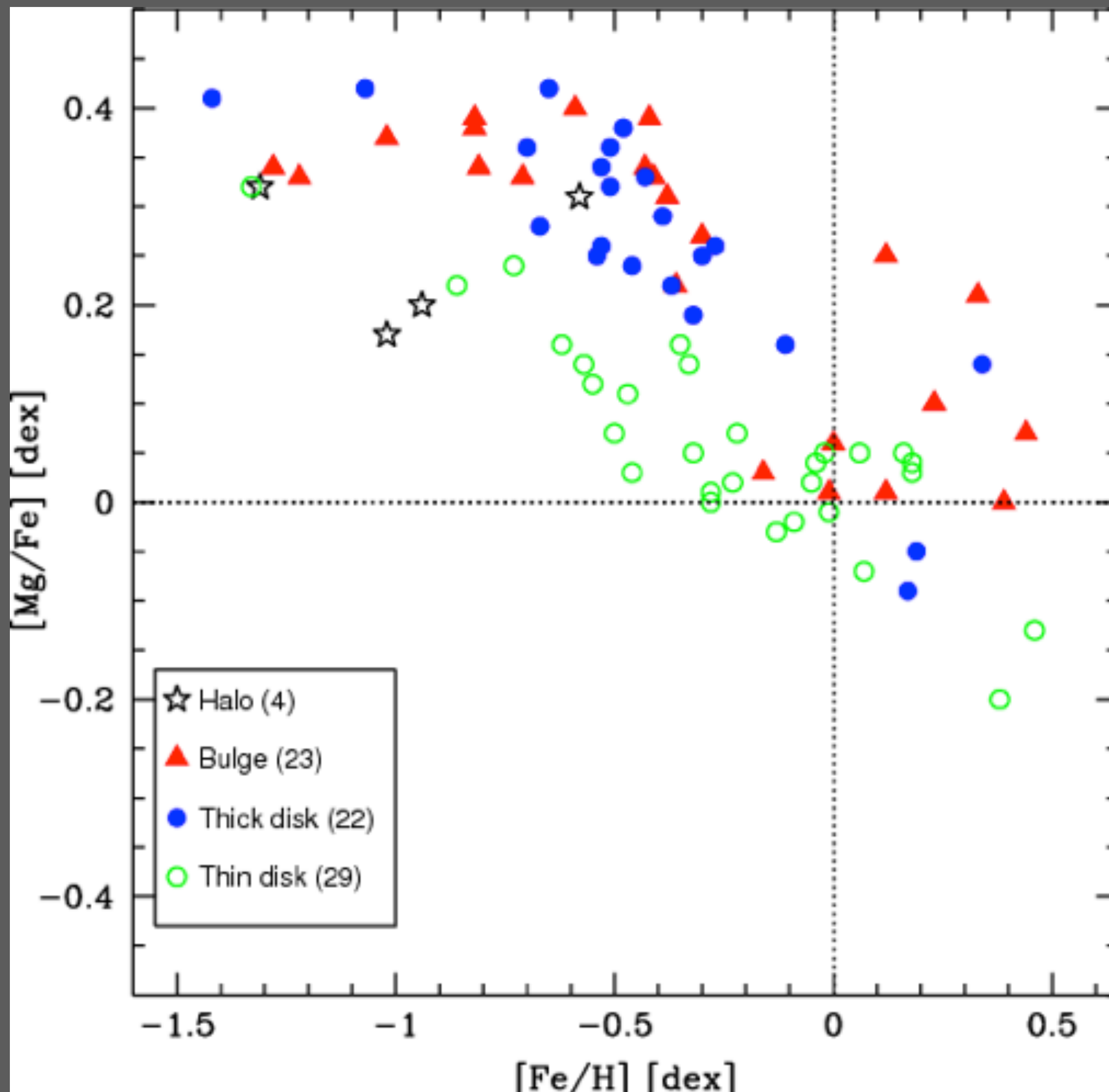

Sobre a formação do bojo da Galáxia

de Alves-Brito et al. 2010

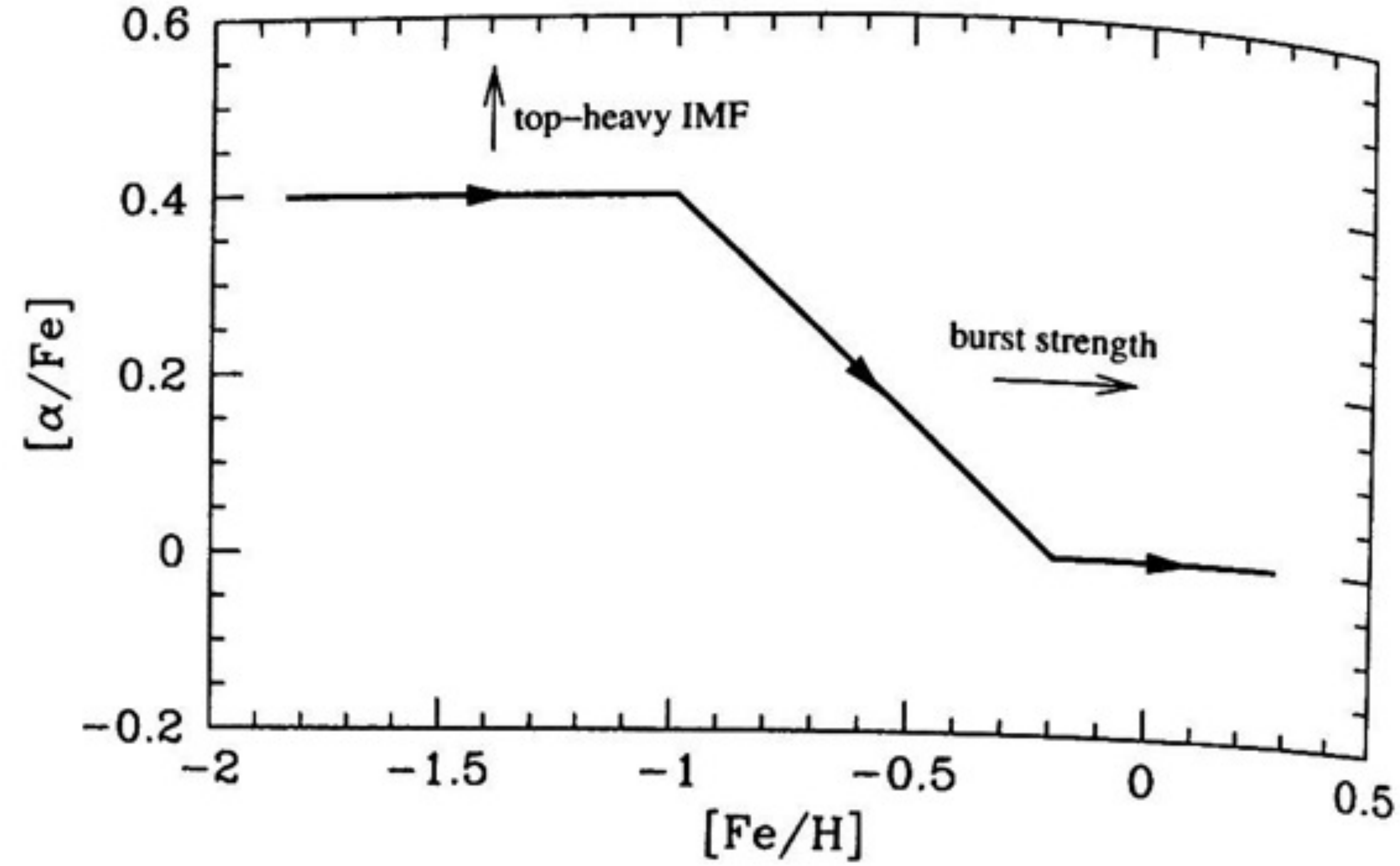

Fig. 10.10. A schematic of the chemical enrichment pattern of the ISM for a single coeval burst of star formation. Time advances along the thick curve as indicated by the arrows. The thin arrows indicate the impact of making the IMF more top-heavy and of increasing the strength of the burst.

$$\log\left(\frac{\Delta t}{\mathrm{Gyr}}\right) \approx 1.2 - 6[\alpha/\mathrm{Fe}]$$

(Thomas et al., 2005).

Em resumo…

Relação entre alpha/Fe e duração da formação estelar

Modelos de evolução química

- Parte-se de algum framework para a origem do gás em galáxias: cosmológico ou 'prompt initial enrichment'

- Quando as estrelas se formam, podem acontecer 3 caminhos genéricos:
    - estrelas de baixa massa (< 1Msun) tem tempos de vida tão longos que não contribuem para o enriquecimento do meio, estas "prendem" o gás e são objetos "arqueológicos" da abundância do meio primordial
    - estrelas de massa intermediária (entre 1 e 9 Msun) passam por vários processos de dredge-up em que C, N, He, Li e elementos-s são processados, parcialmente expelidos no meio por meio de ventos estelares ou nebulosas planetárias. Sistemas binários de estrelas nesse regime podem resultar em SN Ia, que contribuem substancialmente para a nucleossíntese de ferro.

Modelos de evolução química

- estrelas de alta massa (> 9 Msun) completam sua evolução em menos de 10^8 anos e terminam como SN II (ou não) ejetando diversos elementos no meio, incluindo os do processo r. Várias dessas estrelas passam por fases de mixing e perda de massa durante sua vida (Wolf Rayet stars, luminous blue variables, circumstellar shells), contribuindo com CNO.

Principais ingredientes

- Condições iniciais (massa e metalicidade do gás inicial, taxa de acresção)
- Prescrições dos produtos finais da evolução estelar (quais estrelas ejetam quanto de sua massa na forma de quais metais depois de quanto tempo? trajetórias evolutivas, yields estelares, perdas de massa por ventos…)
- Função de Massa Inicial
- Modelo para a taxa de formação estelar (SFR) em função do tempo, massa do gás, densidade do gás, etc…
- Modelos/hipóteses/prescrições para qualquer outro efeito relevante fora o nascimento e morte de estrelas: mixing do ISM, efeitos dinâmicos, trocas de gás com o meio intergaláctico…

The ESO Large Programme “First Stars”

P. Bonifacio, J. Andersen, S.M. Andrievsky, B. Barbuy, T.C. Beers, E. Caffau, R. Cayrel, E. Depagne, P. François, J.I. González Hernández, C.J. Hansen, F. Herwig, V. Hill, S.A. Korotin, H.-G. Ludwig, P. Molaro, B. Nordström, B. Plez, F. Primas, T. Sivarani, F. Spite and M. Spite

1 Introduction

In ESO period 65 (April–September 2000) the large programme 165.N-0276, led by Roger Cayrel, began making use of UVES at the Kueyen VLT telescope. Known within the Team and outside as “First Stars”, it was aimed at obtaining high resolution, high signal-to-noise ratio spectra in the range 320 nm–1000 nm for a large sample of extremely metal-poor (EMP) stars identified from the HK objective prism survey [3, 4]. The goal was to use these spectra to determine accurate atmospheric parameters and chemical composition of these stars which are among the oldest objects amenable to our detailed study. Although these stars are not the first generation of stars they must be very close descendants of the first generation. One may hope to gain insight on the nature of the progenitors from detailed information on the descendants.

The ESO Large Programme "First Stars"

Author, Title Query Results

adsabs.harvard.edu/cgi-bin/nph-abs_connect?db_key=AST&db_key=PRE&qform=AST&arxiv_sel=astro-ph&sim_query=YES&ned_

The G-dwarf problem in the Galaxy | Author, Title Query Results

paulartcoelho@gmail.com | my Account | Sign off

SAO/NASA Astrophysics Data System (ADS)

Query Results from the ADS Database

Go to bottom of page

Retrieved **200** abstracts, starting with number **1**. Total number selected: **1038**.

Sort options

#	Bibcode / Authors	Score / Title	Date	List of Links / Access Control Help
1	2013A&A...550A.122S Siqueira Mello, C.; Spite, M.; Barbuy, B.; Spite, F.; Caffau, E.; Hill, V.; Wanajo, S.; Primas, F.; Plez, B.; Cayrel, R.; and 7 coauthors	1.000 First stars. XVI. HST/STIS abundances of heavy elements in the uranium-rich metal-poor star CS 31082-001	02/2013	A E F X D R C S U
2	2011A&A...534A..60B Barbuy, B.; Spite, M.; Hill, V.; Primas, F.; Plez, B.; Cayrel, R.; Spite, F.; Wanajo, S.; Siqueira Mello, C.; Andersen, J.; and 5 coauthors	1.000 First stars. XV. Third-peak r-process element and actinide abundances in the uranium-rich star CS31082-001	10/2011	A E F D R C S U
3	2011A&A...528A...9S Spite, M.; Caffau, E.; Andrievsky, S. M.; Korotin, S. A.; Depagne, E.; Spite, F.; Bonifacio, P.; Ludwig, H.-G.; Cayrel, R.; François, P.; and 8 coauthors	1.000 First stars. XIV. Sulfur abundances in extremely metal-poor stars	04/2011	A E F X D R C S U
4	2011A&A...527A..65H	1.000	03/2011	A E F X D R C S U

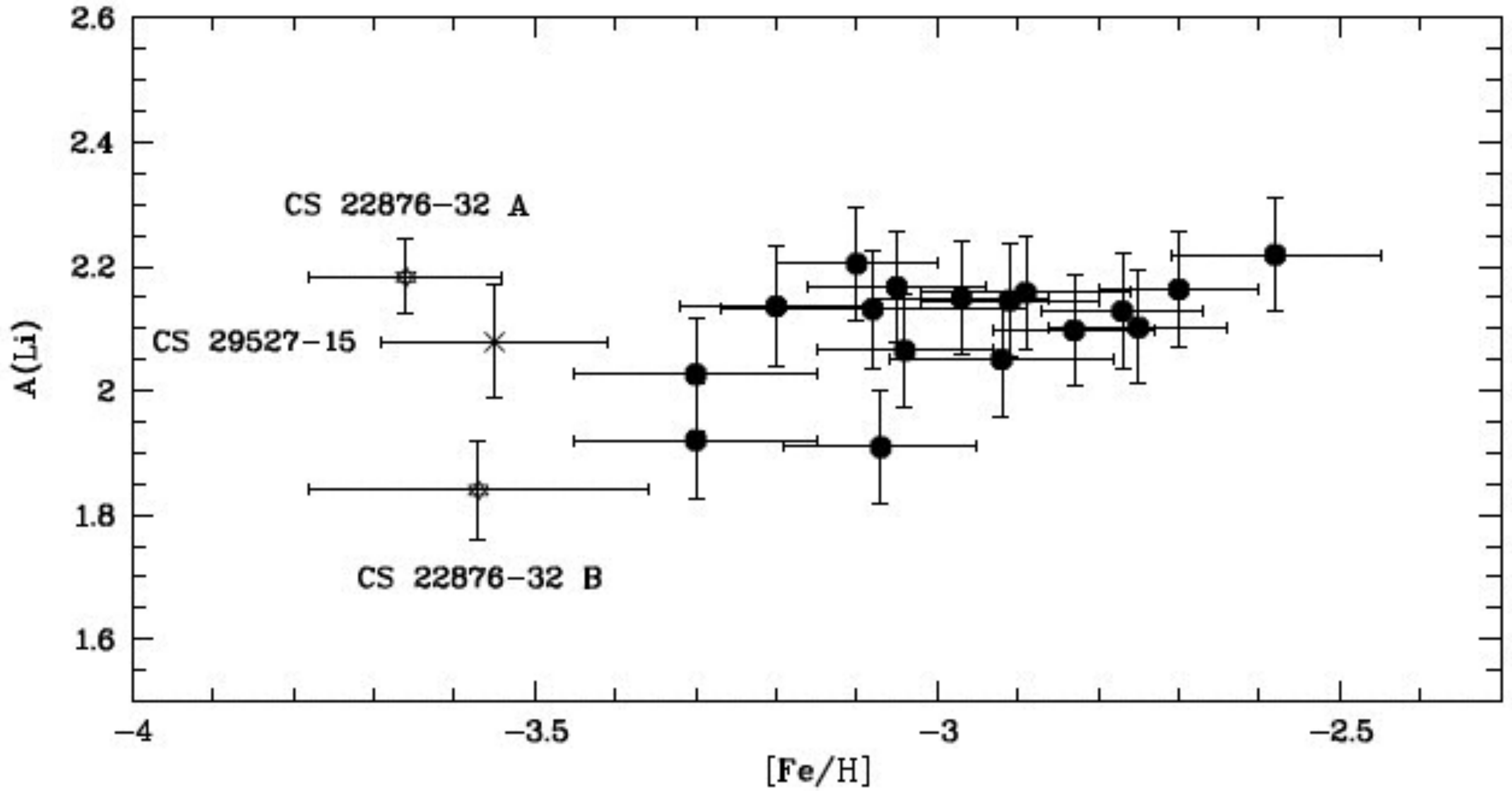

Fig. 1. The Spite plateau at the lowest metallicities as portrayed by the "First Stars" data. The stars whose names are labelled are binaries, for CS 22876-32 an orbital solution is available and the analysis has been done taking properly into account the veiling and Li in both components has been measured, for CS22957-15 this has not been possible, due to the lack of the necessary data, however the correction for the veiling is likely not very large.

The Spite Plateau

A(Li) stars ~ 2.1 vs A(Li) BB ~ 2.64

a) the Spite plateau does not represent the primordial abundance? or

b) primordial nucleosynthesis did not proceed as assumed in the "standard" model?

Closed-box model *ou* Simple 1-zone model

- van den Bergh (1962) e Schimdt (1963)
- Dedução em Mo, van den Bosch, White p. 488, Pagel 251
- Hipóteses:
  - sistema é isolado e massa é conservada (não há inflows ou outflows)
  - o gás é sempre homogêneo no tempo (mixing instantâneo)
  - o gás primordial tem Z = 0 (nucleossíntese primordial)
  - IMF e yields (de elementos primários) são constantes no tempo
- logo nos primeiros modelos foi identificado o “G-dwarf problem”
- ainda assim esses modelos são úteis em “situações controladas"

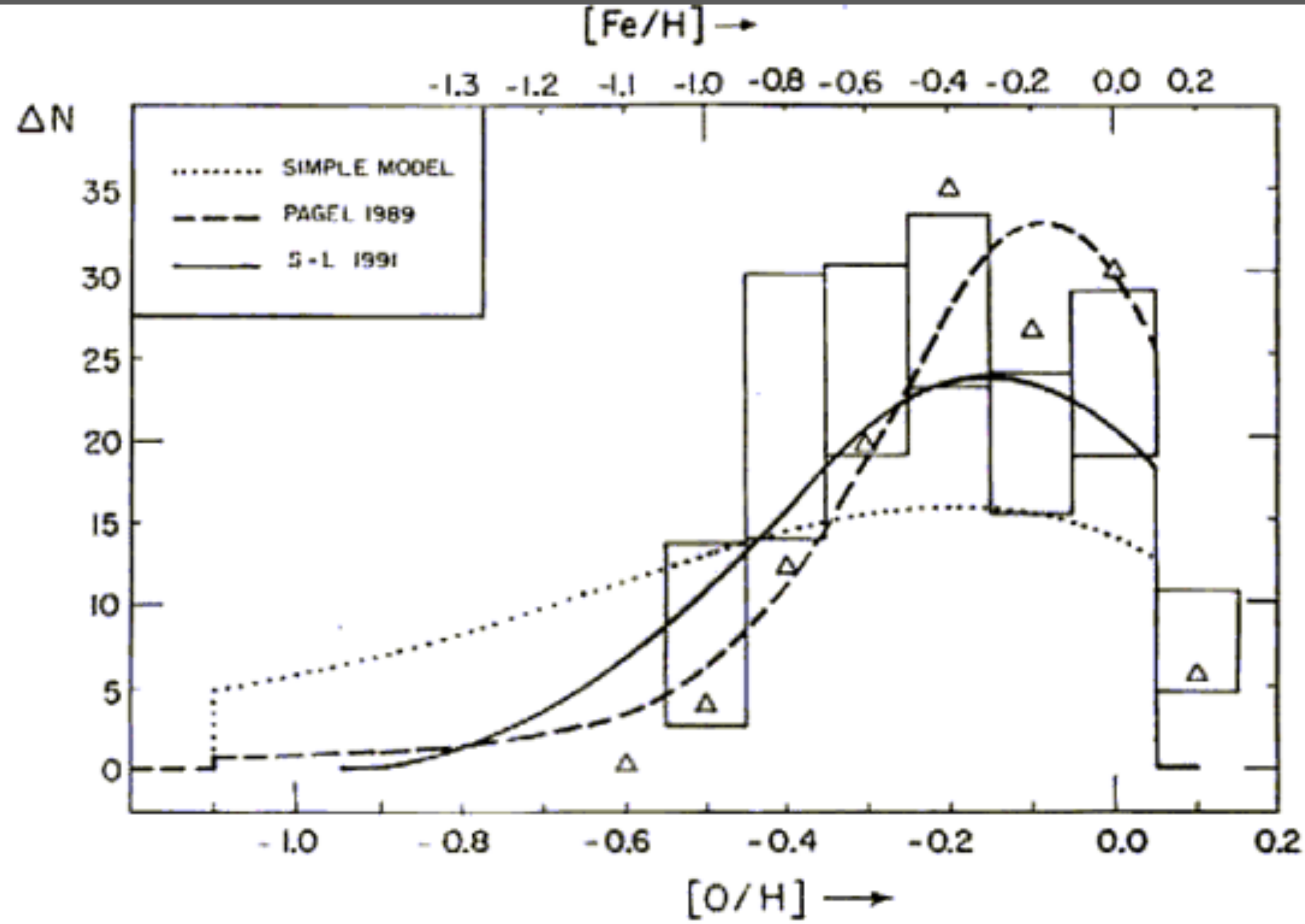

Fig. 8.19. Distribution function of oxygen abundances of 132 G-dwarfs in the solar cylinder, binned in intervals of 0.1 in [O/H]. Triangles show the data points after Pagel (1989ab), based on a reanalysis of those discussed by Pagel & Patchett (1975), and boxes show lower and upper limits based on a new discussion of the dependence of the scale height on age and metallicity by Sommer-Larsen (1991a). The dotted curve shows predictions of an instantaneous Simple model with an initial enrichment [O/H] = −1.1 from the halo. The other model curves are discussed below. After B.E.J. Pagel, 'Abundances in Galaxies', in H. Oberhummer (ed.), *Nuclei in the Cosmos*, p. 98, Fig. 9. ©Springer-Verlag Berlin Heidelberg 1991.

THE ASTROPHYSICAL JOURNAL, 477:765–780, 1997 March 10

THE CHEMICAL EVOLUTION OF THE GALAXY: THE TWO-INFALL MODEL

C. CHIAPPINI,[1,2] F. MATTEUCCI,[1] AND R. GRATTON[3]

Received 1996 April 23; accepted 1996 October 3

ABSTRACT

We present a new chemical evolution model for the Galaxy that assumes two main infall episodes, for the formation of the halo–thick disk and thin disk, respectively. We do not try to take into account explicitly the evolution of the halo since our model is better suited for computing the evolution of the disk (thick plus thin), but we implicitly assume that the timescale for the formation of the halo was of the same order as the timescale for the formation of the thick disk. The formation of the thin disk is much longer than that of the thick disk, implying that the infalling gas forming the thin disk comes not only from the thick disk but mainly from the intergalactic medium.

The timescale for the formation of the thin disk is assumed to be a function of Galactocentric distance, leading to an inside-out picture for the Galaxy's building. The model takes into account the most up-to-date nucleosynthesis prescriptions and adopts a threshold in the star formation process, which naturally produces a hiatus in the star formation rate at the end of the thick-disk phase, as suggested by recent

Relaxando o
Closed-box model…

Abstract

- We present a new chemical evolution model for the Galaxy that assumes two main infall episodes, for the formation of the halo and thick disk and thin disk, respectively.
- The formation of the thin disk is much longer than that of the thick disk, implying that the infalling gas forming the thin disk comes not only from the thick disk but mainly from the intergalactic medium.
- The model results are compared with an extended set of observational constraints both for the solar neighborhood and for the whole disk. Among these constraints, the tightest is the metallicity distribution of the G-dwarf stars, for which new data are now available. Our model fits these new data very well.
- In order to reproduce most of these constraints, a timescale of <=1 Gyr for the (halo) thick disk and of 8 Gyr for the thin disk formation in the solar vicinity are required.

Aim

- The aim of this paper is to test the two-infall chemical evolution model with respect to the maximum number of available observational constraints in the Galaxy.

2. OBSERVATIONAL CONSTRAINTS

A good model of the chemical evolution of the Galaxy should reproduce a number of constraints that is greater than the number of free parameters. Therefore it is very important to choose a high-quality set of observational data to be compared with model predictions. Our set of constraints includes

1. The relative number of thin-disk and metal-poor stars (halo plus part of the thick-disk stars) in the solar cylinder;
2. Type I and Type II supernova rates at the present time;
3. Solar abundances;
4. Present-day gas fraction;
5. Age-metallicity relation;
6. Present-day infall rate;
7. Metallicity distributions for disk and metal-poor stars;
8. The variation in the relative abundances of the most common chemical elements;
9. Radial profiles for the star formation rate and gas mass density; and
10. Radial abundance gradients.

Outline

- Introduction
- Observational Constraints (how the model will be tested)
- The Model (assumptions and ingredients)
- Results (both predictions of the model and comparison to observations)
- Discussion and Conclusions

Highlights

- This model assumes two distinct infall episodes : during the first the thick disk is formed, and during the second, delayed relative to the first, the thin disk forms.
- The thin disk starts forming roughly at the end of the thick-disk phase. In this model, the material accreted by the Galactic thin disk comes mainly from extragalactic sources, and this is the fundamental difference […]
- For the thin disk, we assume a radially varying $\tau_D(r)$, which implies that the inner parts of the thin disk are built much more rapidly than the outer ones. In other words, we are dealing with an inside-out picture, as suggested by previous models […]
- $\tau_D(r)$ = timescale for mass accretion in the think-disk component

G-dwarf

- Stellar Metallicity Distribution: An important constraint on chemical evolution models is the metallicity distribution of G dwarfs for the solar vicinity. The G-dwarf metallicity distribution is representative of the chemical enrichment of the Galaxy, since these stars have lifetimes greater than or equal to the age of the Galaxy, and hence can provide a complete record of the chemical evolutionary history.

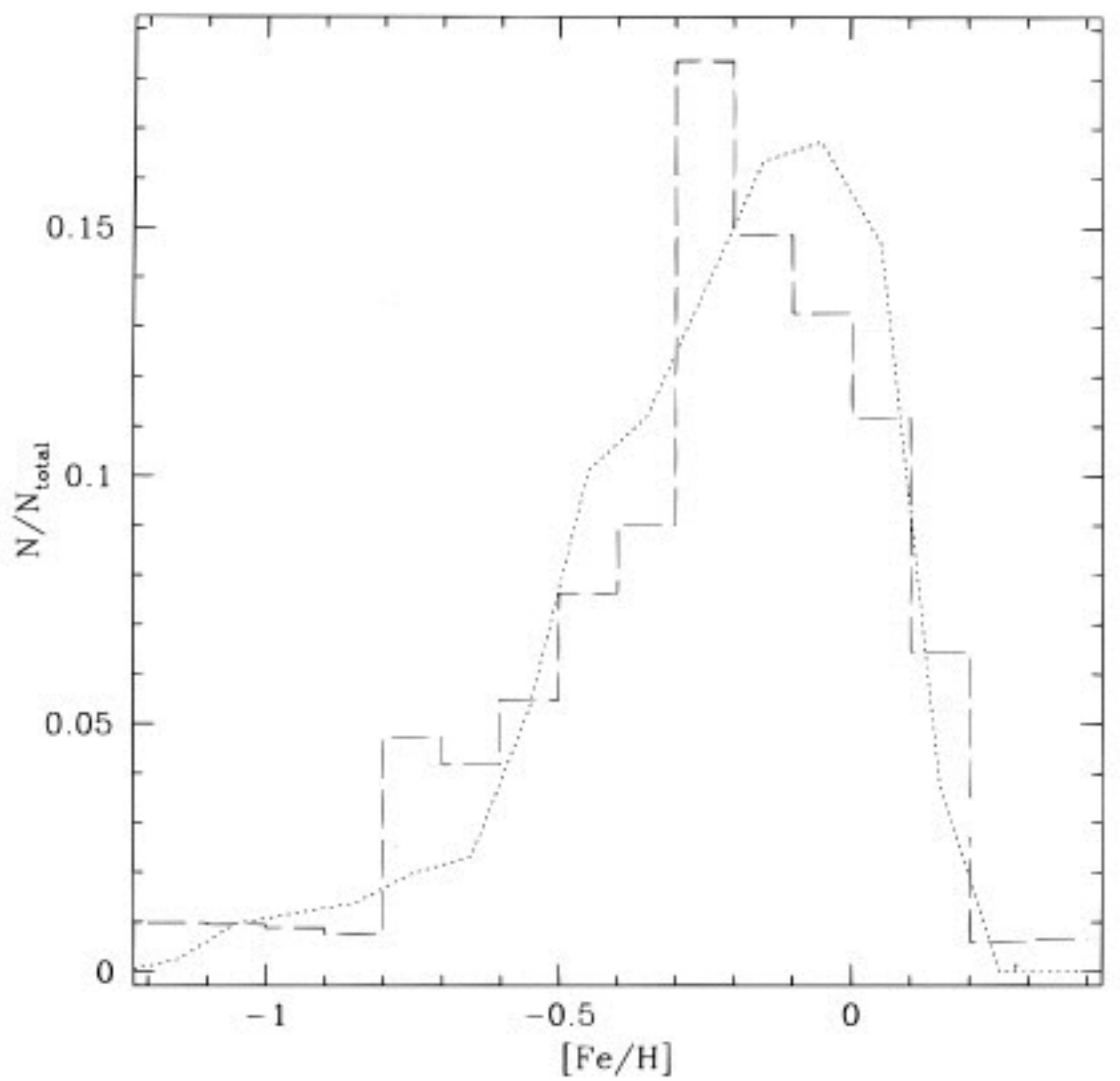

FIG. 7.—G-dwarf metallicity distribution in the solar vicinity predicted by model A. The data are from Rocha-Pinto & Maciel (1996).

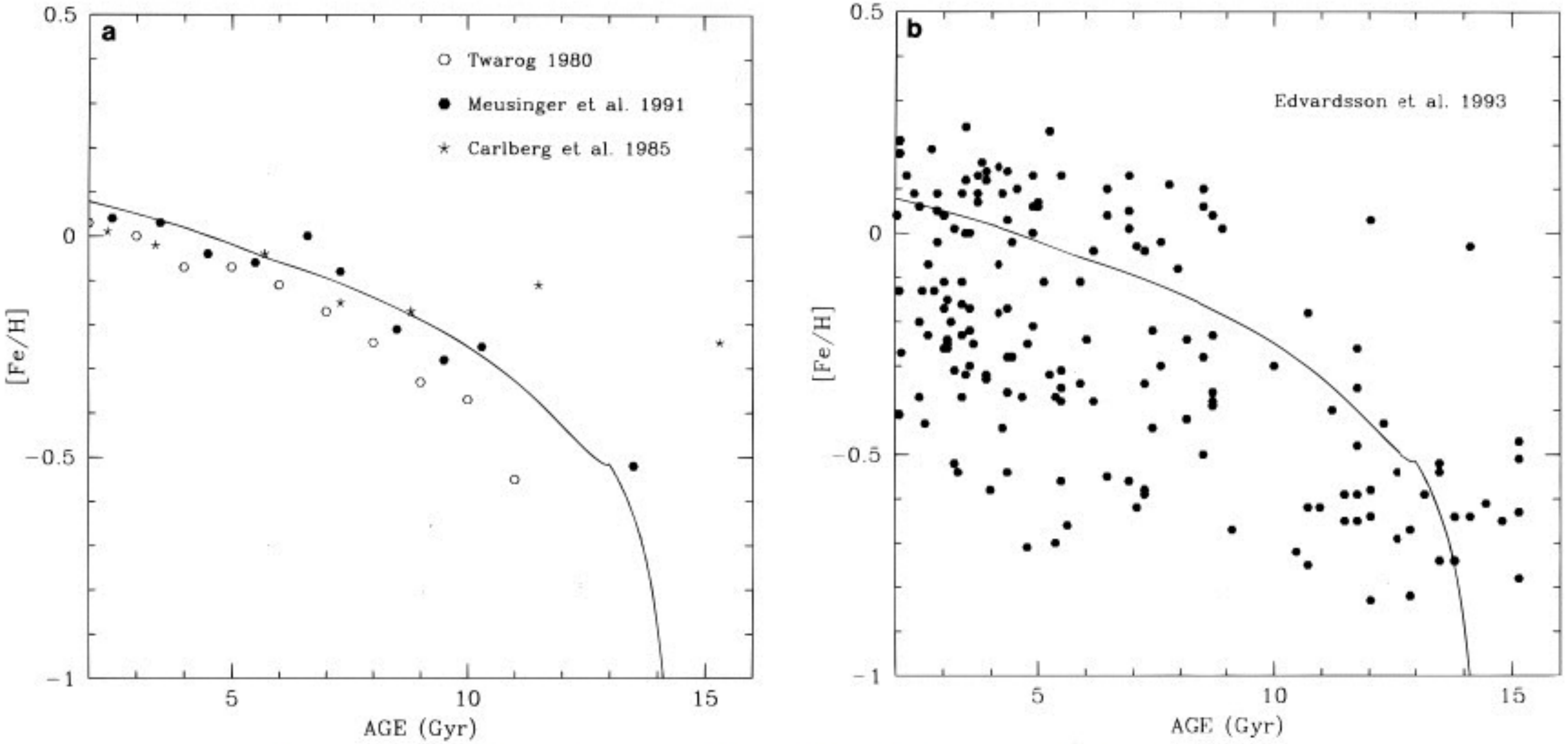

FIG. 1.—Age-metallicity relation for two different data sets. The curve shows the best model prediction.

Comparação com observações

2.4. *Relative Abundances*

Another important constraint is the behavior of the α-to-iron ratio as a function of iron. While the α-elements (O, Ne, Mg, Si, Ca, etc.) are produced only by Type II SNs (which have high-mass progenitors with short lifetimes), most of the iron is produced by Type Ia SNs, which are believed to be the result of the explosion of C-O white dwarfs in binary systems. Iron release from Type Ia SNs begins not before several times 10^7 yr after the birth of a stellar generation, and the bulk of restitution takes up to some gigayears, depending on the assumptions about the binary system's characteristics, explosion mechanism, and star formation rate (SFR). Therefore the delayed arrival of the iron produced by Type Ia SNs is responsible for the observed decrease in the [α/Fe] ratio as a function of the iron abundance in the solar vicinity (Greggio & Renzini 1983; Matteucci & Greggio 1986; MF89). Recently, Gratton et al. (1996)

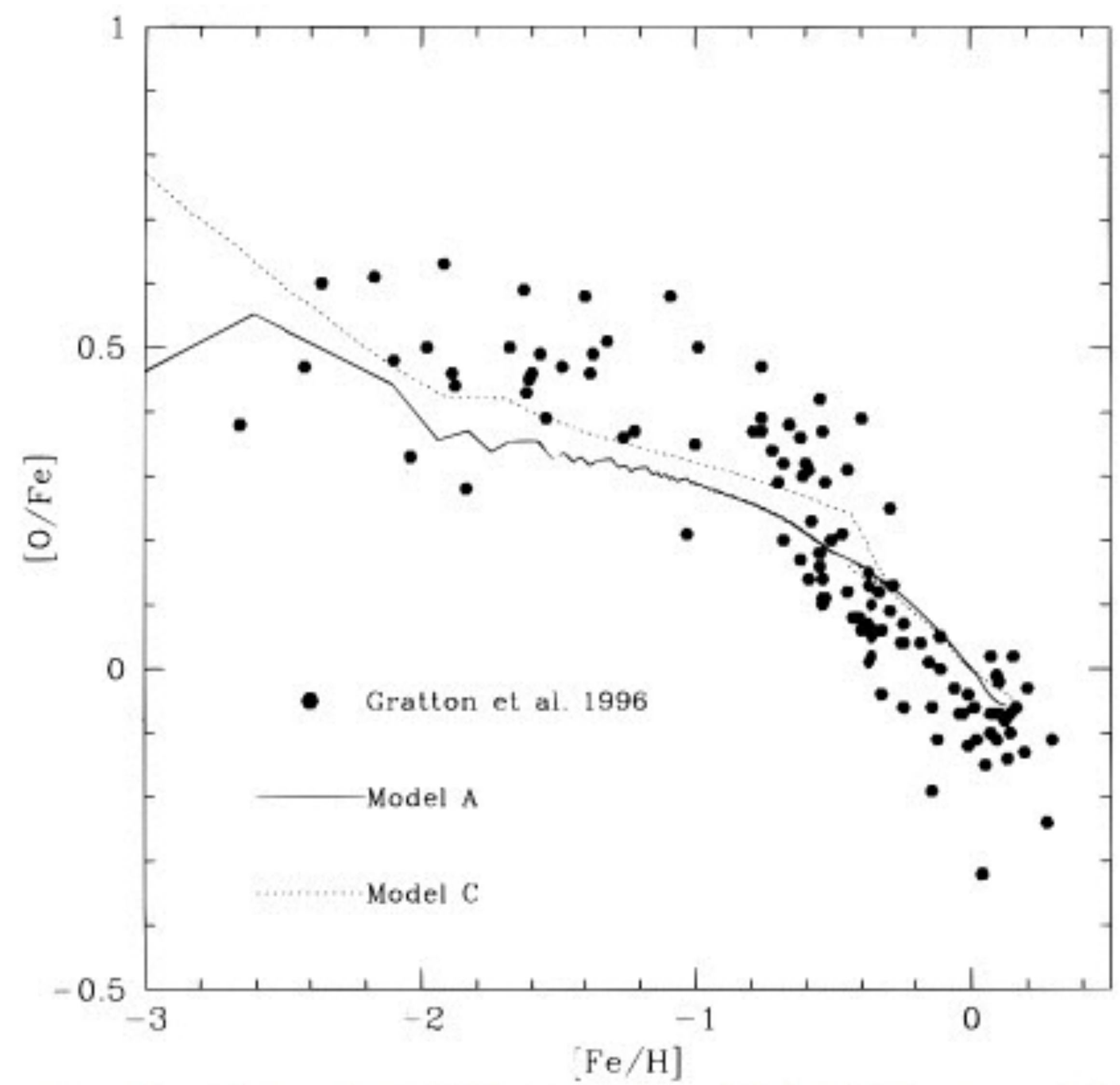

FIG. 3.—[O/Fe] vs. [Fe/H] behavior for model A (*solid line*) and model C (*dotted line*).

Comparação com observações

Predictions

- The resulting star formation rate is shown in Figure 4, for model A, where the threshold effect is clear during the thick-disk phase and also at the end of the thin disk's evolution.

4.3. *The Star Formation History*

As already mentioned in § 3, we adopt a threshold in the star formation rate, which is responsible for the behavior shown in Figure 4. According to this threshold, star formation stops when a surface gas density of 7 $M_{\odot}$ pc^{-2} is reached. This means that star formation can have an intermittent behavior regulated by the surface gas density. In fact, after the threshold is reached and star formation stops, the dying stars continue to restore gas into the interstellar medium, and therefore, sooner or later, the surface gas density will again be above the threshold and star formation will restart.

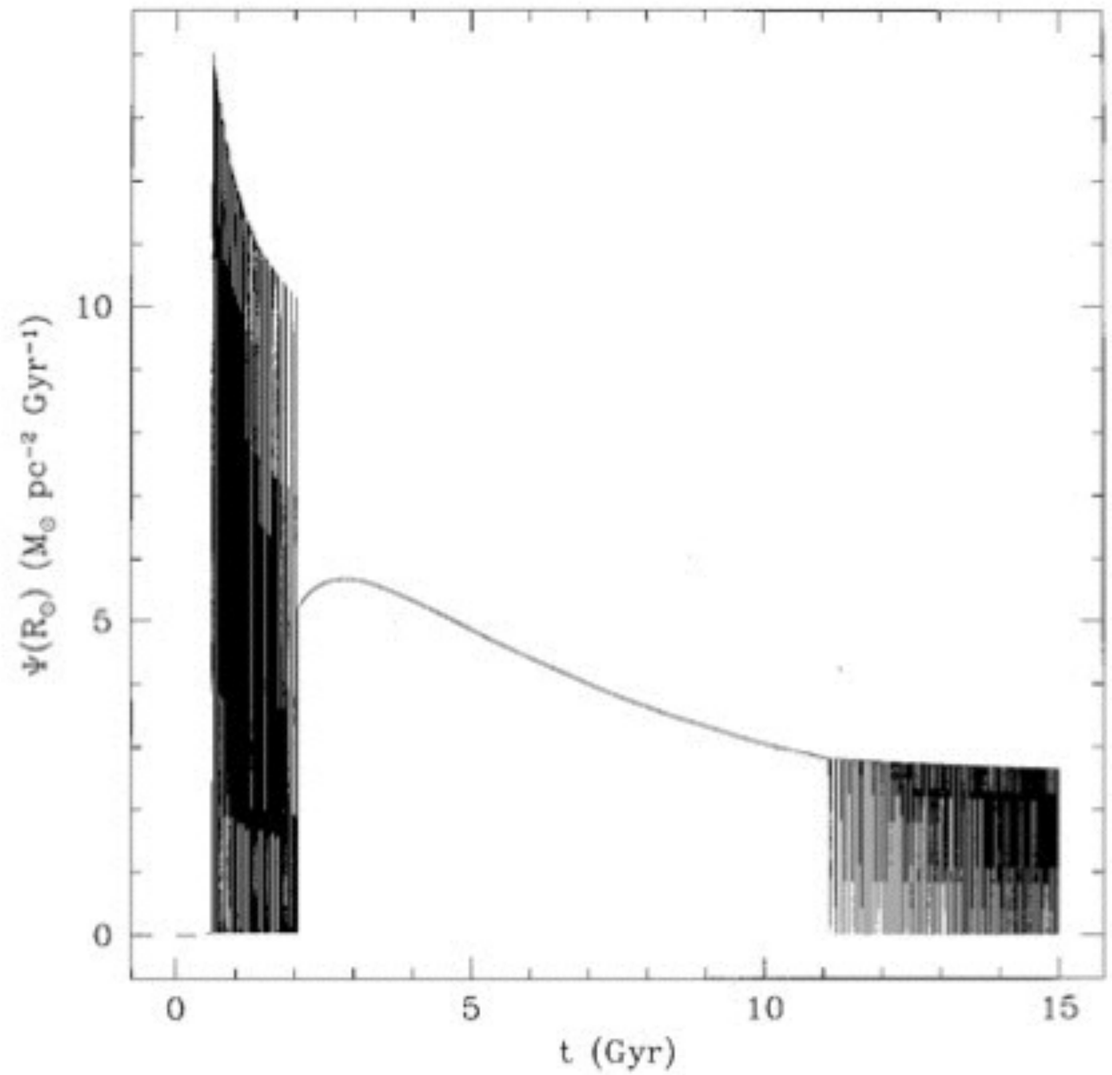

FIG. 4.—Temporal evolution of the star formation rate as predicted by model A for the solar vicinity.

2.1. *Solar Abundances*

The solar abundances should represent the chemical composition of the interstellar medium (ISM) in the solar neighborhood at the time of the Sun's formation (4.5 Gyr ago). However, Cunha & Lambert (1993) showed that the abundance of oxygen in the Orion Nebula is smaller by a factor of 2 than the solar value (Anders & Grevesse 1989), at variance with the increase of the metal abundances in the Galaxy with time as predicted by the chemical evolution models. Thus it is not clear whether the solar composition should be considered as representative of the local ISM 4.5 Gyr ago, a possibility being that the Sun was born in a region closer to the Galactic center and then moved to the present region. It should also be noted that the elemental abundances are uncertain. As discussed by Timmes et al. (1995), given the uncertainties involved, abundance values falling within a factor of 2 inside the observed values can be considered as being in agreement with the solar data.

4. RESULTS

We ran a large number of models for the solar vicinity and the whole disk, varying the star formation rate parameters (i.e., k and ν) and also the timescales for the thick- and thin-disk formation (i.e., τ_T and τ_D). A positively surprising result is that very few combinations of such parameters lead to an agreement with the considered set of observational constraints. Table 2 presents the results of the models of Table 1 compared with the current observational quantities, for the solar vicinity. We remind the reader that model A is our best model.

It is clear from our models that, in order to obtain a reasonable number of metal-poor stars and simultaneously fit the metallicity distribution of the solar vicinity, it is necessary to decouple the evolution of the (halo) thick disk from that of the thin disk.

Outras discussões interessantes

Modelos quimio-dinâmicos (chemo-dynamical)

- Iniciados por Larson (1976) e Tinsley & Larson (1978)
- Em cima dos outros ingredientes já mencionados, um modelo quimio-dinâmico segue a evolução dinâmica das estrelas com simulação de N-corpos e a evolução do gás com hidrodinâmica (ex. SPH).

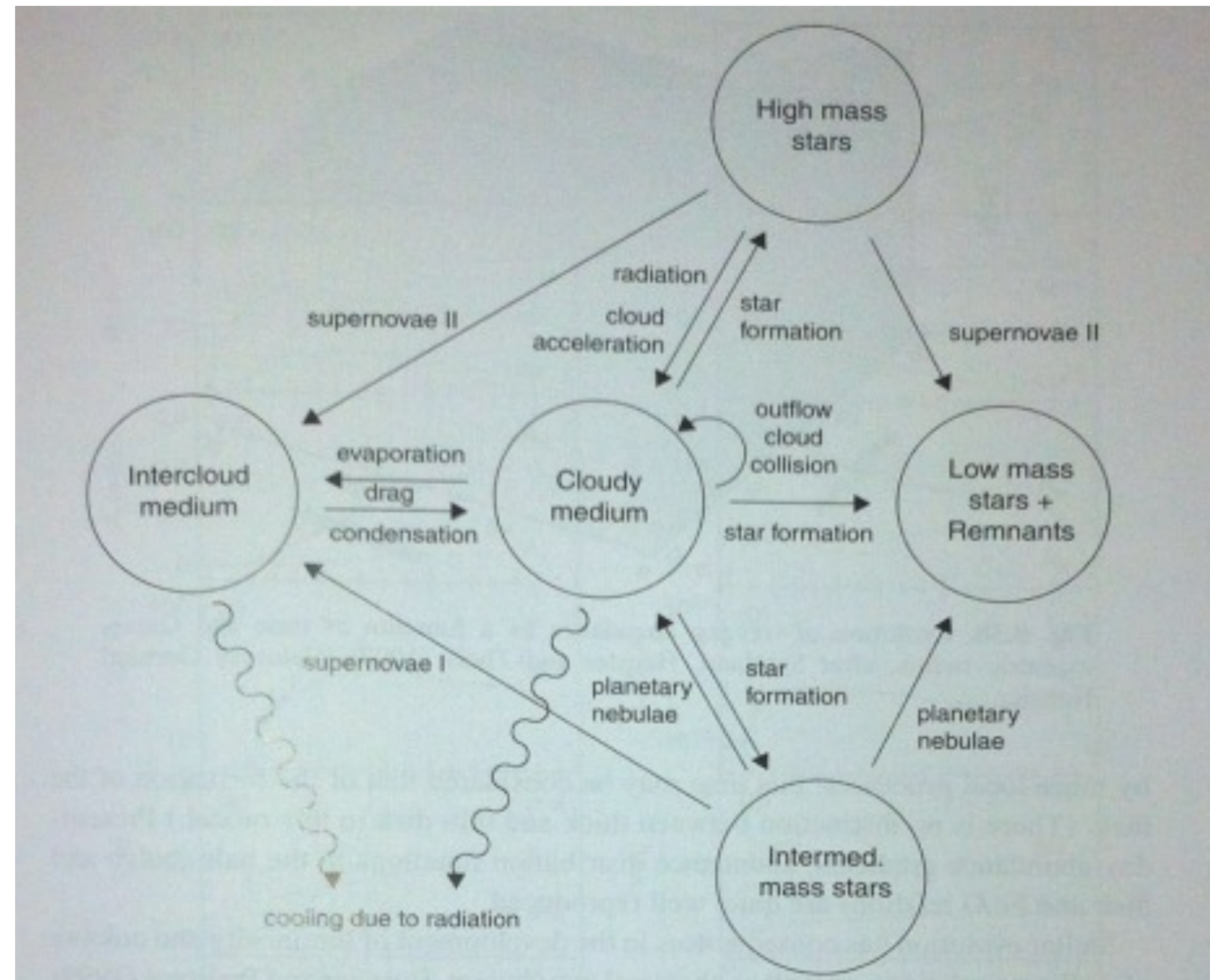

Fig. 8.37. The different gaseous and stellar components connected via mass, momentum and energy exchange, with their principal interactions, in the chemo-dynamical model of the Galaxy, after Samland, Hensler and Theis (1997). Courtesy Gerhard Hensler.

Modelos quimio-dinâmicos

- GCD+: to simulate the formation and evolution of the Milky Way.
- three-dimensional tree N-body/smoothed particle hydrodynamics (SPH) code that incorporates self-gravity, hydrodynamics, radiative cooling, star formation, supernova feedback, and metal enrichment and follows the chemical enrichment history of both the stellar and gas components of the system.
- we are studying how the spiral structures are related to the star formation, and how the spiral structures affect the motion of the stars and gas. We will compare these simulations with the upcoming Gaia data, and disentangle the evolution of the Milky Way disk.

Face-on view of star (left) and gas (right) particle distribution in a simulated Milky Way sized disk. (courtesy of Robert Grand)

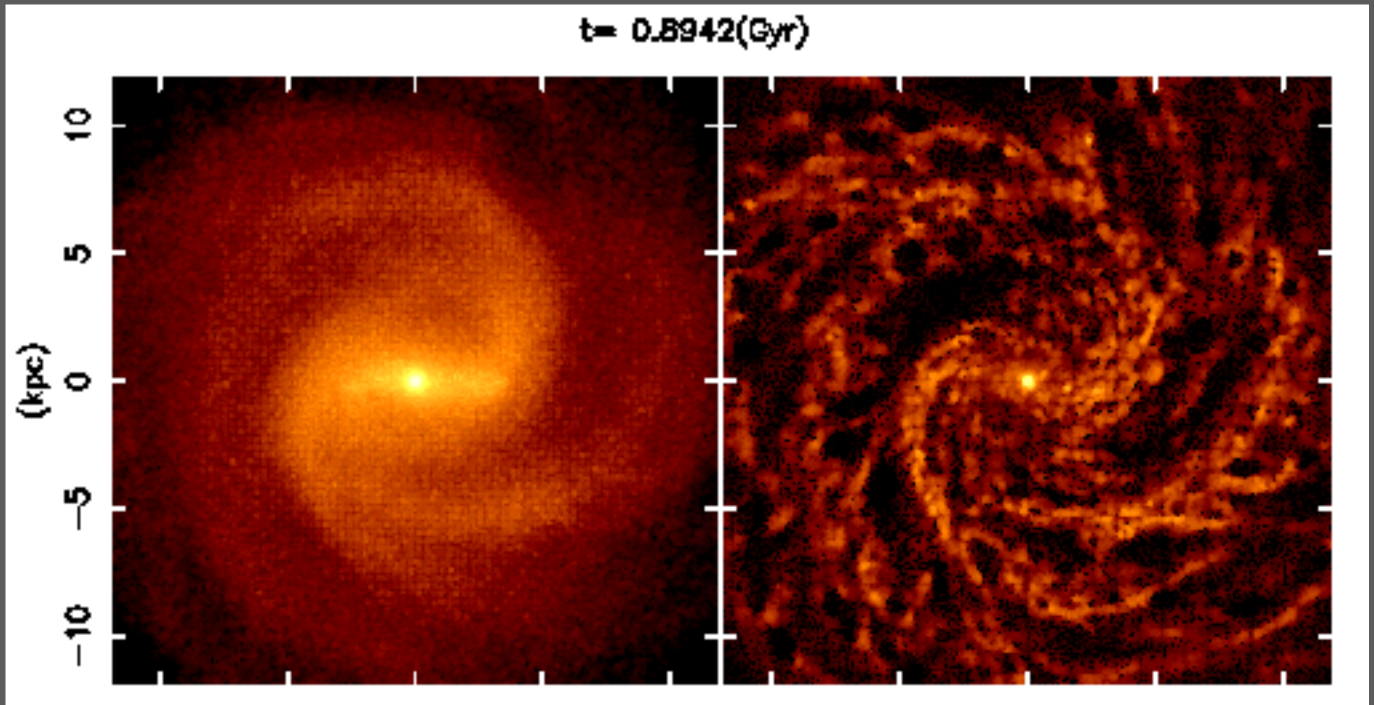

://www.ucl.ac.uk/mssl/astro/research/computation/mwdisk

Modelos quimio-dinâmicos

- GCD+: to simulate the formation and evolution of the Milky Way.
- three-dimensional tree N-body/smoothed particle hydrodynamics (SPH) code that incorporates self-gravity, hydrodynamics, radiative cooling, star formation, supernova feedback, and metal enrichment and follows the chemical enrichment history of both the stellar and gas components of the system.
- we are studying how the spiral structures are related to the star formation, and how the spiral structures affect the motion of the stars and gas. We will compare these simulations with the upcoming Gaia data, and disentangle the evolution of the Milky Way disk.

Face-on view of star (left) and gas (right) particle distribution in a simulated Milky Way sized disk. (courtesy of Robert Grand)

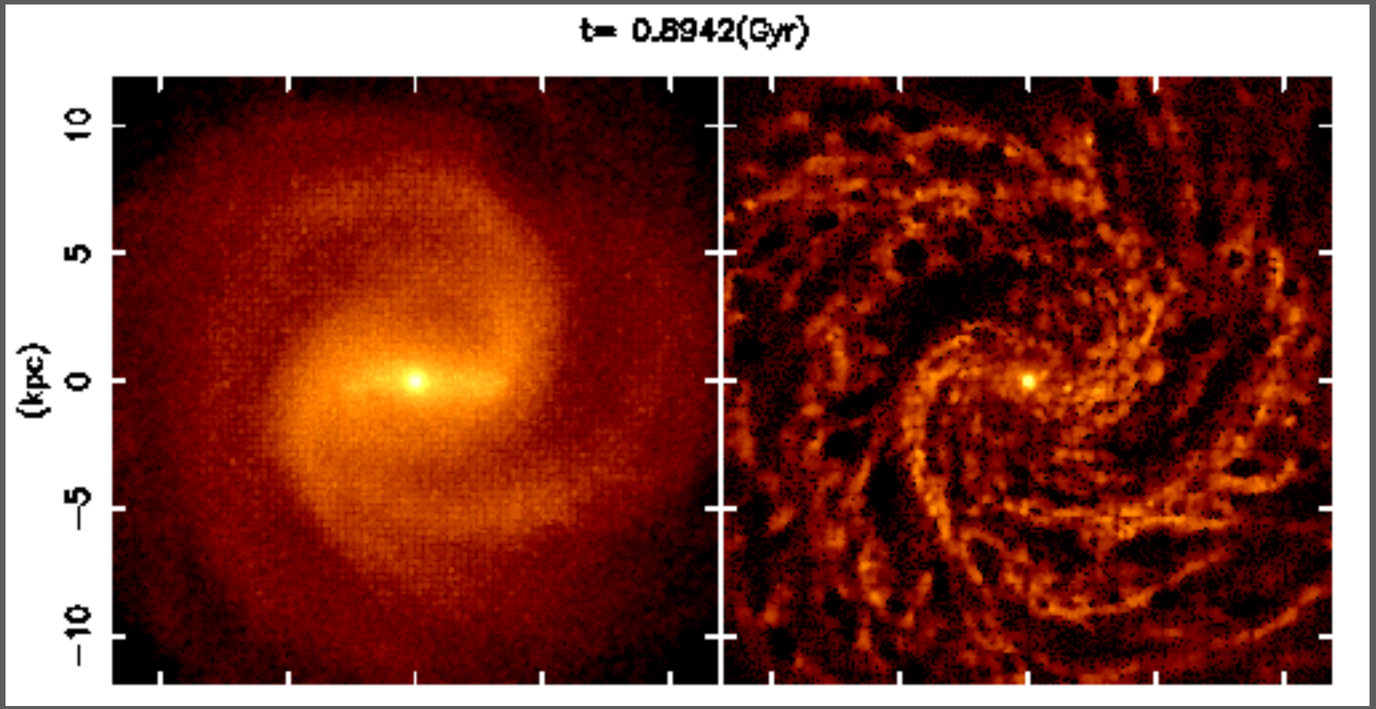

://www.ucl.ac.uk/mssl/astro/research/computation/mwdisk

Evolução química em galáxias anãs

- Galáxias anãs próximas estão classificadas em 4 tipos principais:
    - anãs irregulares (dIrr): as mais comuns, geralmente galáxias sem estrutura com graus variados de formação estelar
    - anãs compactas azuis (BCD): galáxias ricas em H II dominadas por intensa formação estelar e que lembram regiões gigantes de H II em galáxias maiores. A taxa de formação estelar atual pode-se manter por apenas poucos períodos.

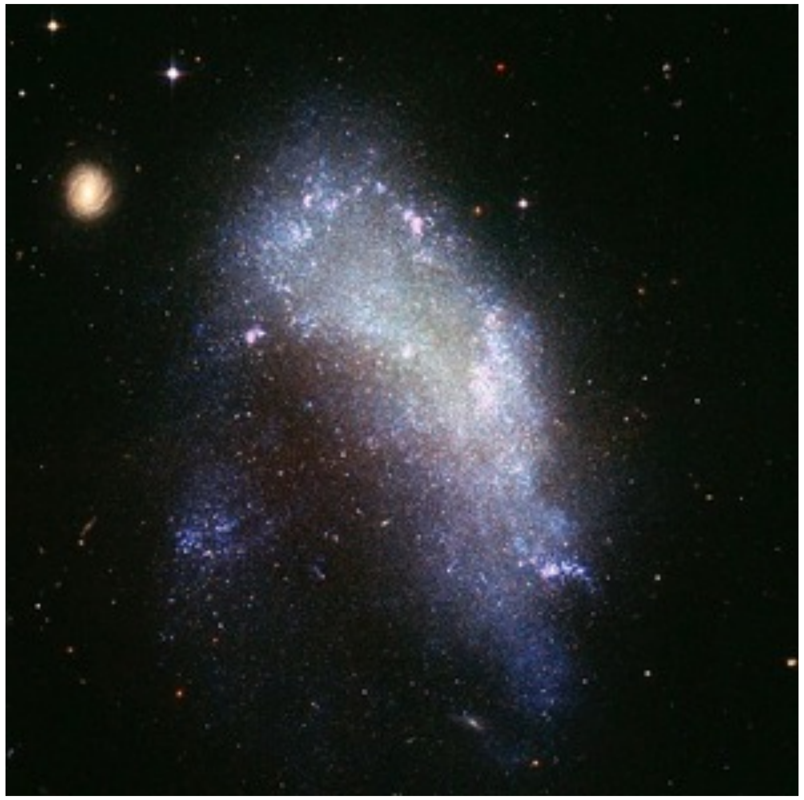

Evolução química em galáxias anãs

- Galáxias anãs próximas estão classificadas em 4 tipos principais (cont.):
  - esferoidais anãs (dSph): galáxias sem gás, com distribuição estelar semelhante a aglomerados globulares mas menos concentradas. Diagramas HR geralmente indicam que vários burts de formação estelar ocorreram no passado.
  - elípticas anãs (dE): estruturalmente semelhantes a elípticas, mais massivas que dSph, e com evidências de formação estelar mais recente.

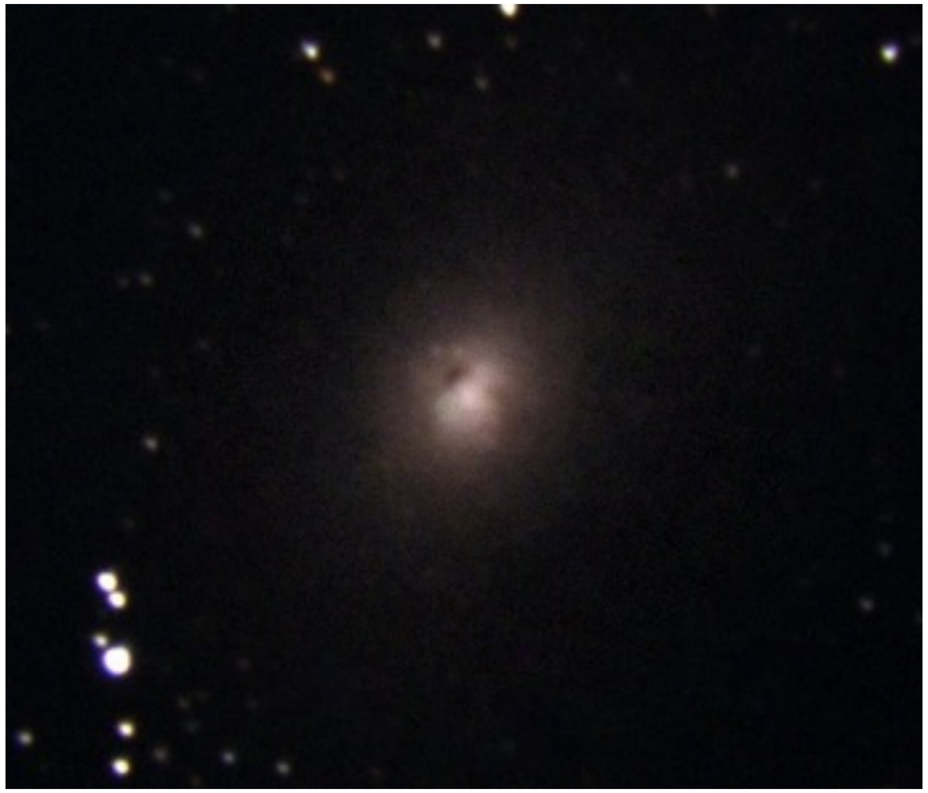

Evolução química em galáxias anãs

- Modelos closed-box podem ser aplicados com relativo sucesso, em particular nos sistemas ricos em gás
- O gás pode ser “expulso" por “terminal winds” ou ram-pressure, se a galáxia pertence a um cluster
- Uma relação estreita foi encontrada entre metalicidade e velocidade de dispersão para as galáxias elípticas (ver a seguir)
- a remoção de gás por um outro processo pode talvez transformar uma anã rica em gás em uma anã elíptica de mesma metalicidade (controverso)

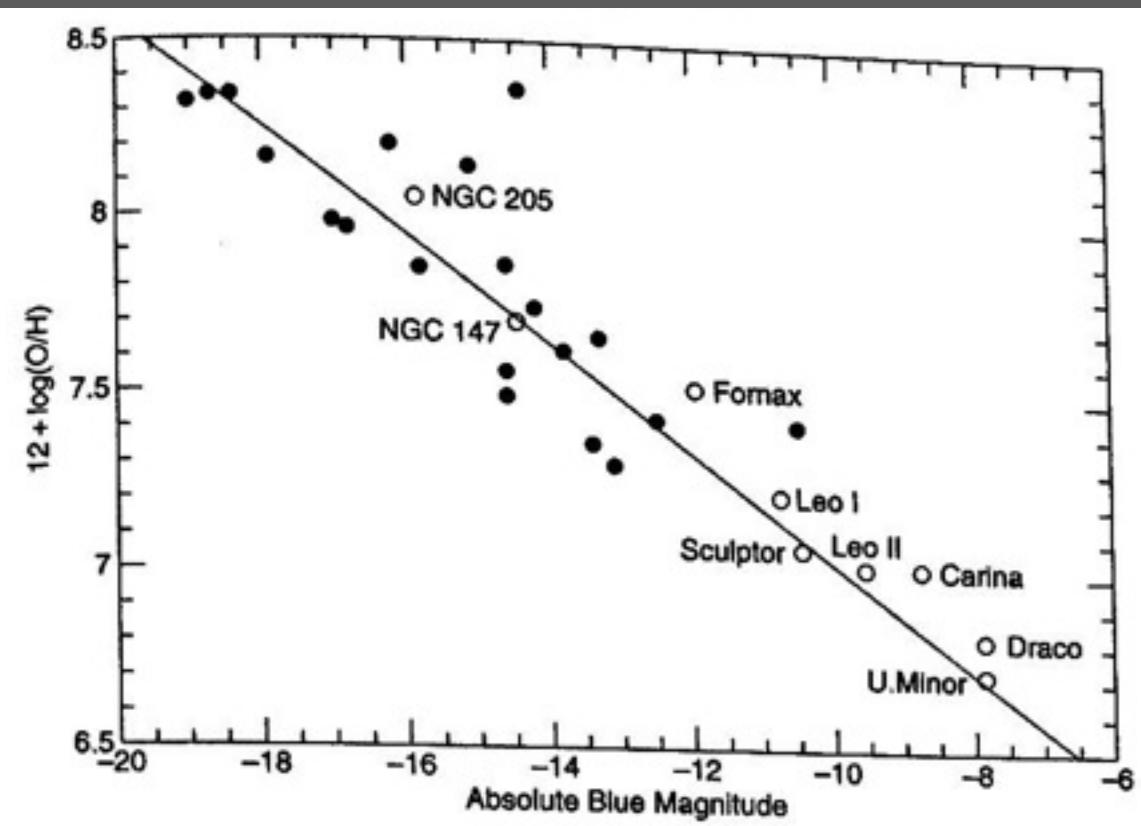

Fig. 11.1. Abundance against absolute magnitude for irregular, dwarf elliptical and dwarf spheroidal galaxies, after Skillman, Kennicutt and Hodge (1989). The vertical scale shows logarithmic oxygen abundances measured in H II regions of irregular galaxies (filled circles), while open circles show ⟨[Fe/H]⟩ + 8.9 for dwarf ellipticals and dwarf spheroidals using [Fe/H] deduced from colours of stars on the giant branch in the HR diagram. The dwarf ellipticals and spheroidals should probably have been plotted up to 0.4 dex higher to convert their mean [Fe/H] into their maximum [Fe/H] so as to be comparable to the young populations represented by H II regions (Richer & McCall 1995); the resulting offset can be attributed to fading after star formation ceased. Courtesy Evan Skillman.

Relação entre anãs ricas em gás e anãs elípticas???

Nuvens de Magalhães

- Devido a sua proximidade, podem ser estudadas através de
  - observação direta das estrelas mais luminosas
  - regiões H II
  - nebulosas planetárias
  - remanescentes de SN

http://apod.nasa.gov/apod/ap130610.html

http://apod.nasa.gov/apod/ap100903.html

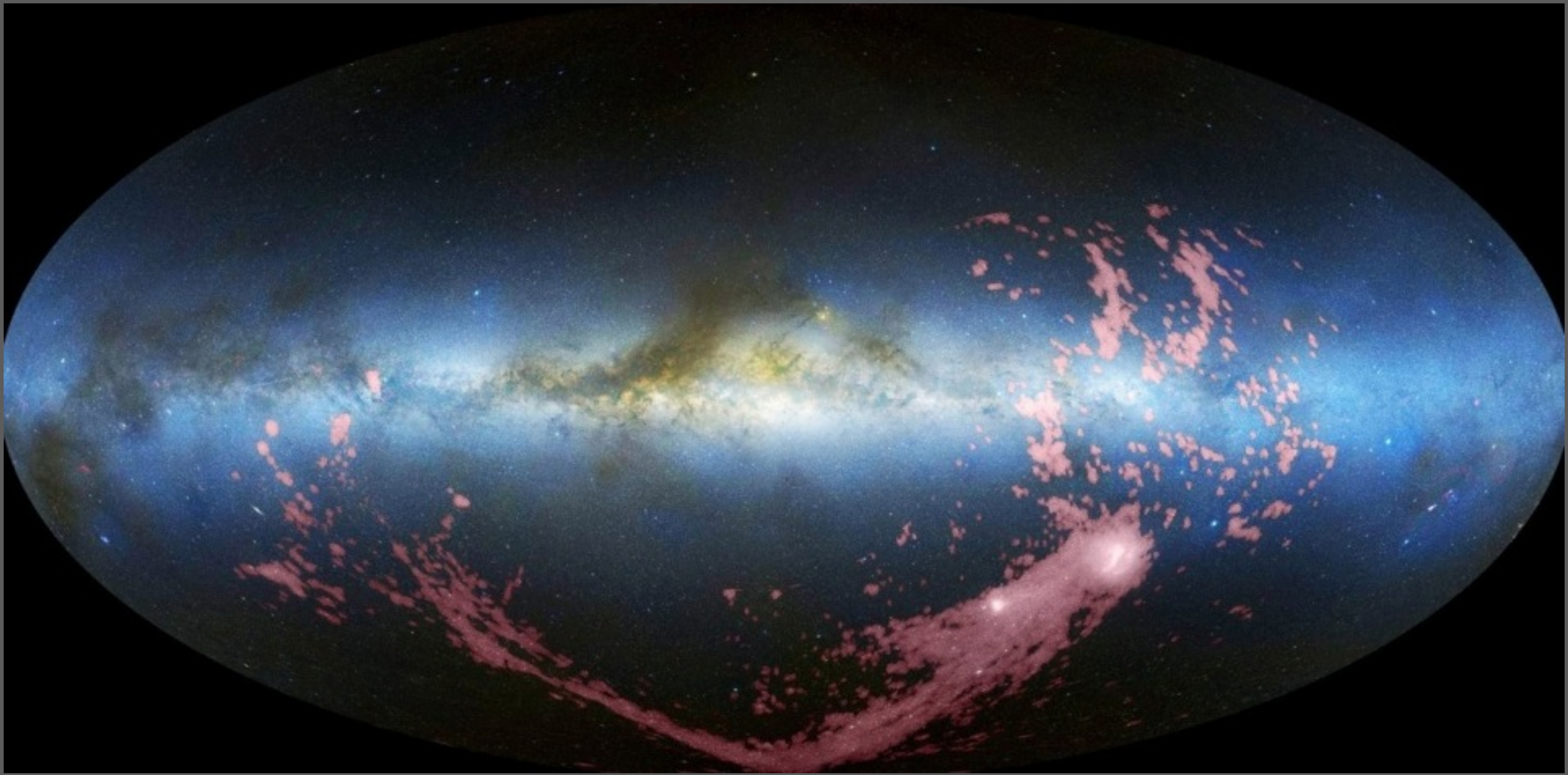

http://apod.nasa.gov/apod/ap130815.html

Magellanic Stream

LMC

- Modelos de evolução química e comparação com dados observacionais
- Existe uma semelhança entre abundâncias químicas medidas na LMC e estrelas anômalas do nosso halo (Nissen & Schuster 97) (escalas de tempo mais longas de formação?)
- abaixo de [Fe/H] = -1.3 há um plato similar ao do halo da MW, indicando produtos puros de SN II

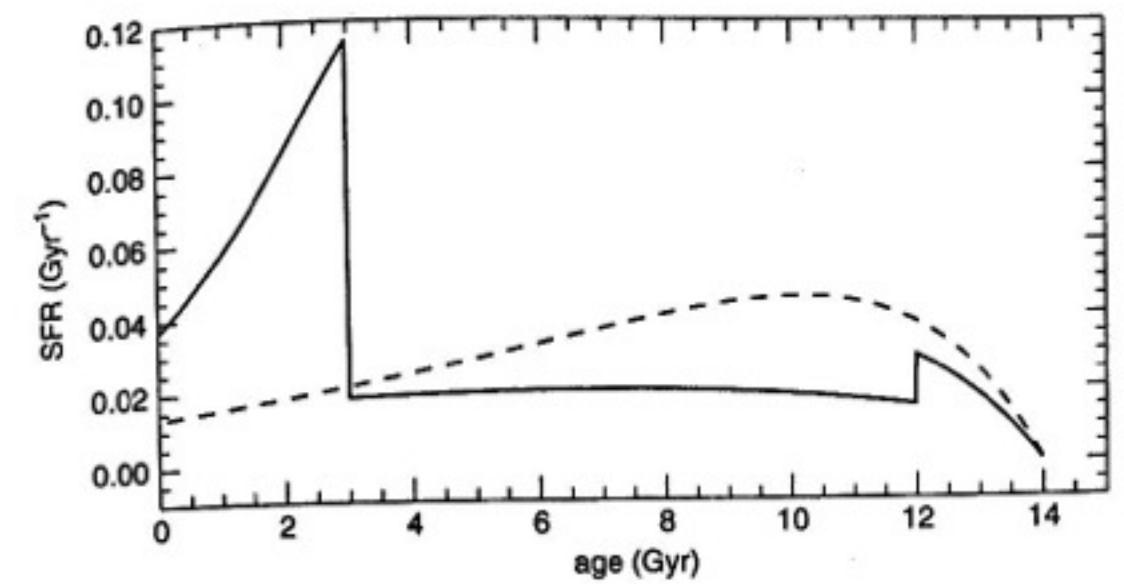

Fig. 11.3. SFR history of the LMC assumed in our models. The full curve shows the bursting model, while the broken curve shows a smooth model with $\omega = 0.18$, compared to $\omega \simeq 0.3$ for the solar neighbourhood. After Pagel and Tautvaišienė (1998).

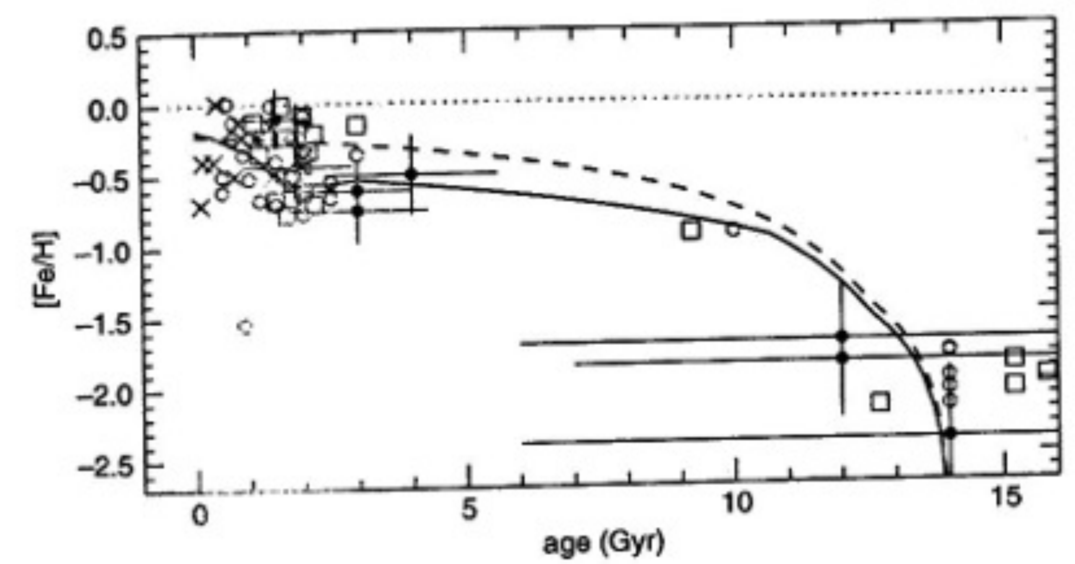

Fig. 11.4. Age–metallicity relation for the LMC, according to the SFR models shown in Fig. 11.3. After Pagel and Tautvaišienė (1998).

Evolução química de galáxias elípticas

- Com exceção das anãs elípticas do grupo local (e da M32!), informação sobre abundâncias em galáxias elípticas só (!) é obtido por cores ou espectros integrados (de populações estelares compostas?)
- A interpretação não é tão óbvia e mais modelagem é necessária (síntese de populações)
- aglomerados globulares tem um papel vital no estudo de elípticas como um "benchmark": podemos estudá-los tanto com observações resolvidas quando integradas
- Convém mencionar a síntese de populações de Bica & Alloin (1986, 1987)
- Índices espectrais são historicamente muito importantes no estudo dessas galáxias
- os parâmetros estruturais das galáxias dinamicamente quentes caem no Plano Fundamental **(Bender, Burstein & Faber 1993)**.

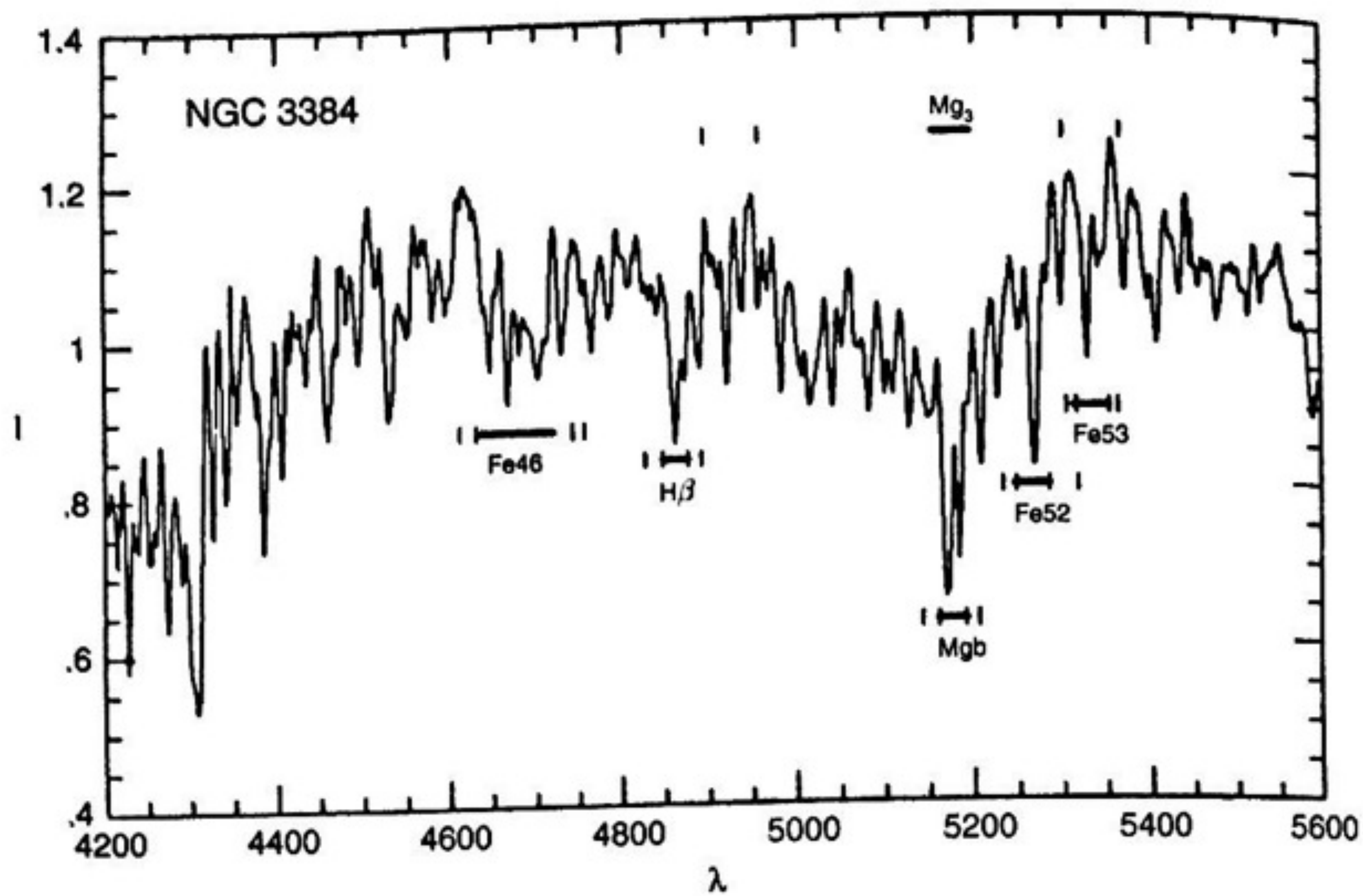

Fig. 3.17. Spectrum of the central region of an S0 galaxy, NGC 3384, showing hydrogen, magnesium and iron spectral features used in the Lick system. The resolution is 3.1 Å ($\sim$ 75 km s^{-1}), compared to a line-of-sight velocity dispersion $\sim$ 140 km s^{-1}. After Fisher, Franx and Illingworth (1996). Courtesy Garth Illingworth.

Índices de Lick

$Mg_2 \sim 0.1\ [Z/Zsun\ t(Gyr)]^{0.41}$
(Bender, Burstein & Faber 1993)

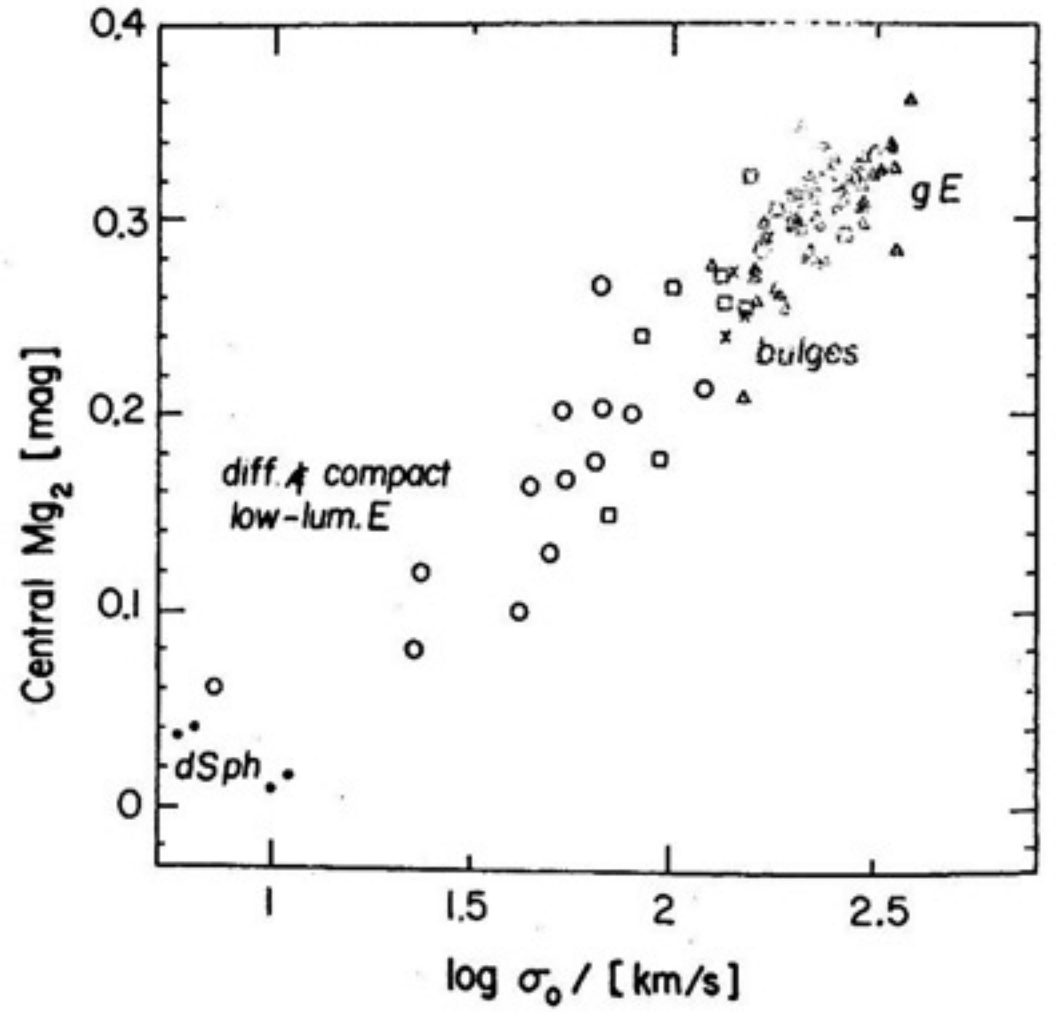

Fig. 11.11. Relation between central Mg_2 index and central velocity dispersion for dynamically hot galaxies. Coding as in Fig. 11.10. Adapted from Bender (1992).

Mg_2 vs σ

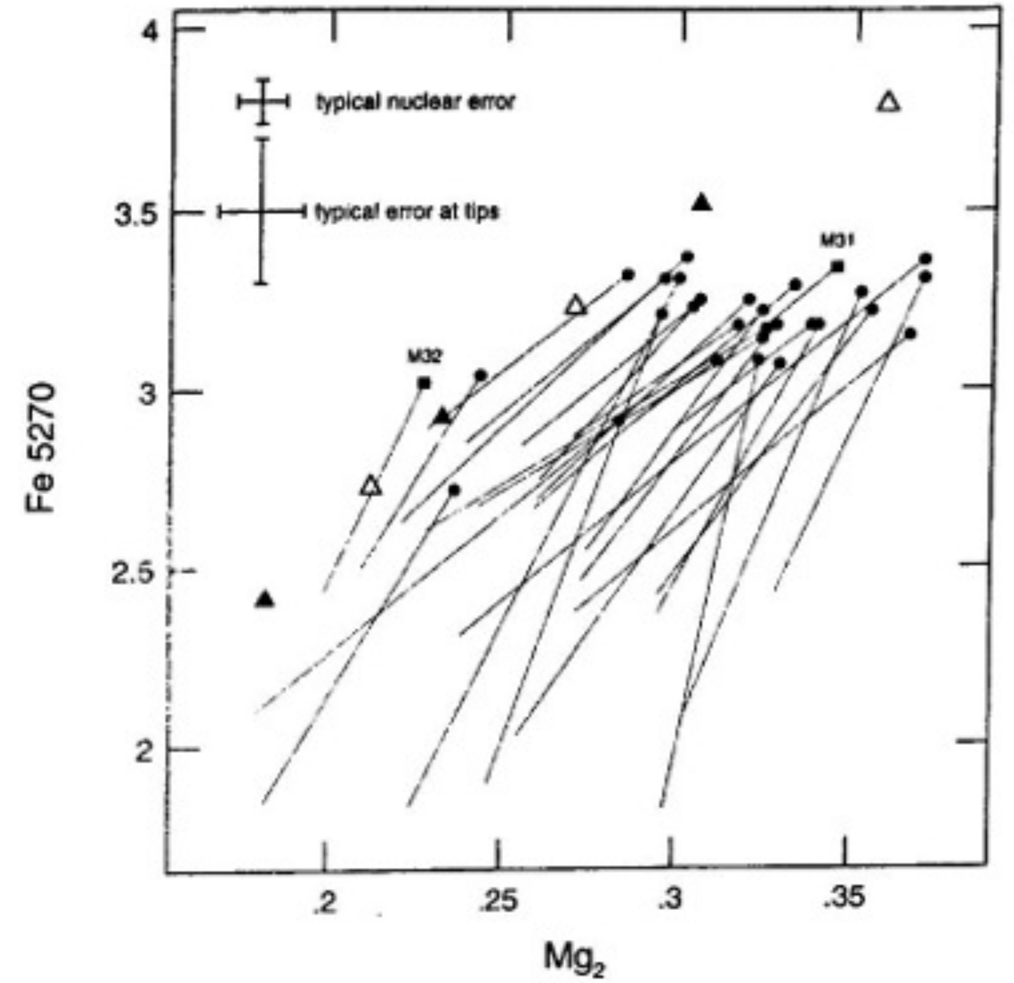

Fig. 11.12. Plot of an iron feature against Mg_2. Filled circles and squares represent the nuclear regions (central 5 arcsec) of elliptical galaxies, while the sloping lines show the mean trend with galactocentric distance in each one. Triangles show model predictions for ages of 9 (solid) and 18 Gyr (open), based on a single burst of star formation, which fit the features in globular clusters and assume [Mg/Fe] = 0. A young model with [Fe/H] = 0 fits the nucleus of M32 quite well, and the predicted trends with metallicity run roughly parallel to several of the observational lines, but the trend among nuclei is not fitted at all. After Worthey, Faber and Gonzalez (1992). Courtesy Guy Worthey.

Razões de [α/Fe]

“Wind models”

- a presença de metais no meio intercluster é uma evidência da existência de ventos (outflow)
- estima-se que as SNs devem ser capazes de acelerar o gás em cerca de 700 km/s, comparável a velocidade de escape de uma galáxia como a MW, se não houverem fontes importantes de cooling.
- Terminal wind ocorre tipicamente em ~2Gyr.

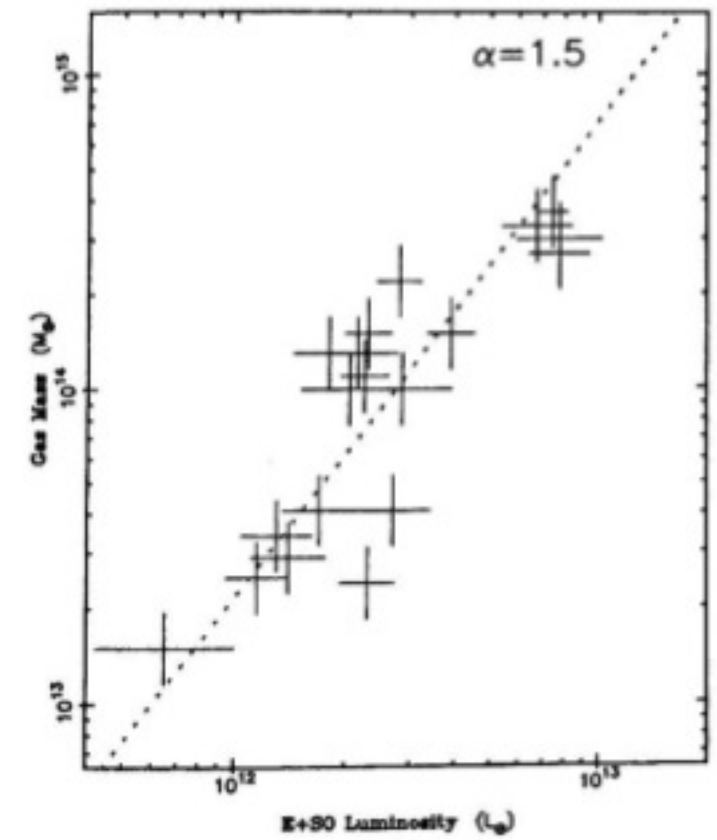

Fig. 11.18. Gas mass in clusters of galaxies plotted against the total luminosity of elliptical and lenticular (S0) galaxies in the cluster. The 1σ error in the slope α is $\pm$0.25. After Arnaud *et al.* (1992). Courtesy Monique Arnaud.

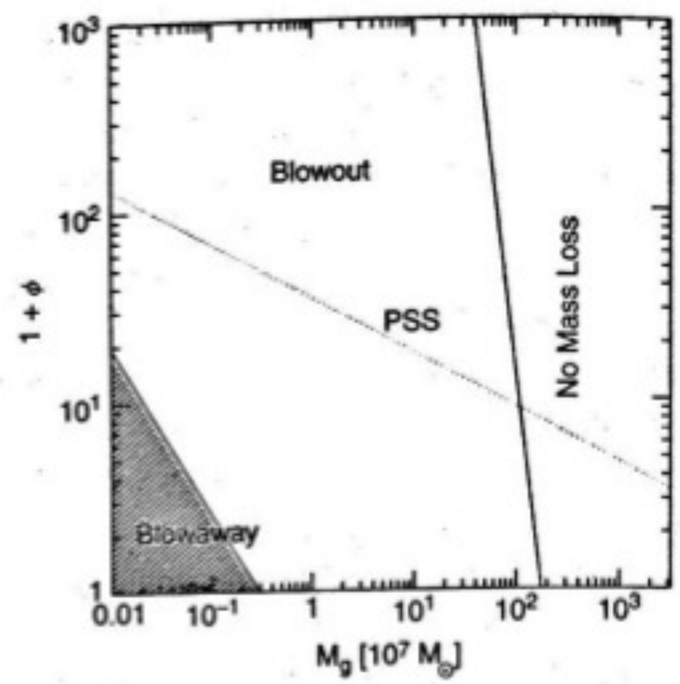

Fig. 11.15. Conditions for gas loss from a galaxy, as a function of gas mass M_g and the ratio ϕ of dark matter to baryons (stars + gas), assuming an energy input of 10^{38} erg s^{-1} and maximum dissipation from cloud–cloud collisions. PSS denotes the relation between ϕ and M_g deduced from observation by Persic, Salucci and Stel (1996). After Ferrara and Tolstoy (2000).

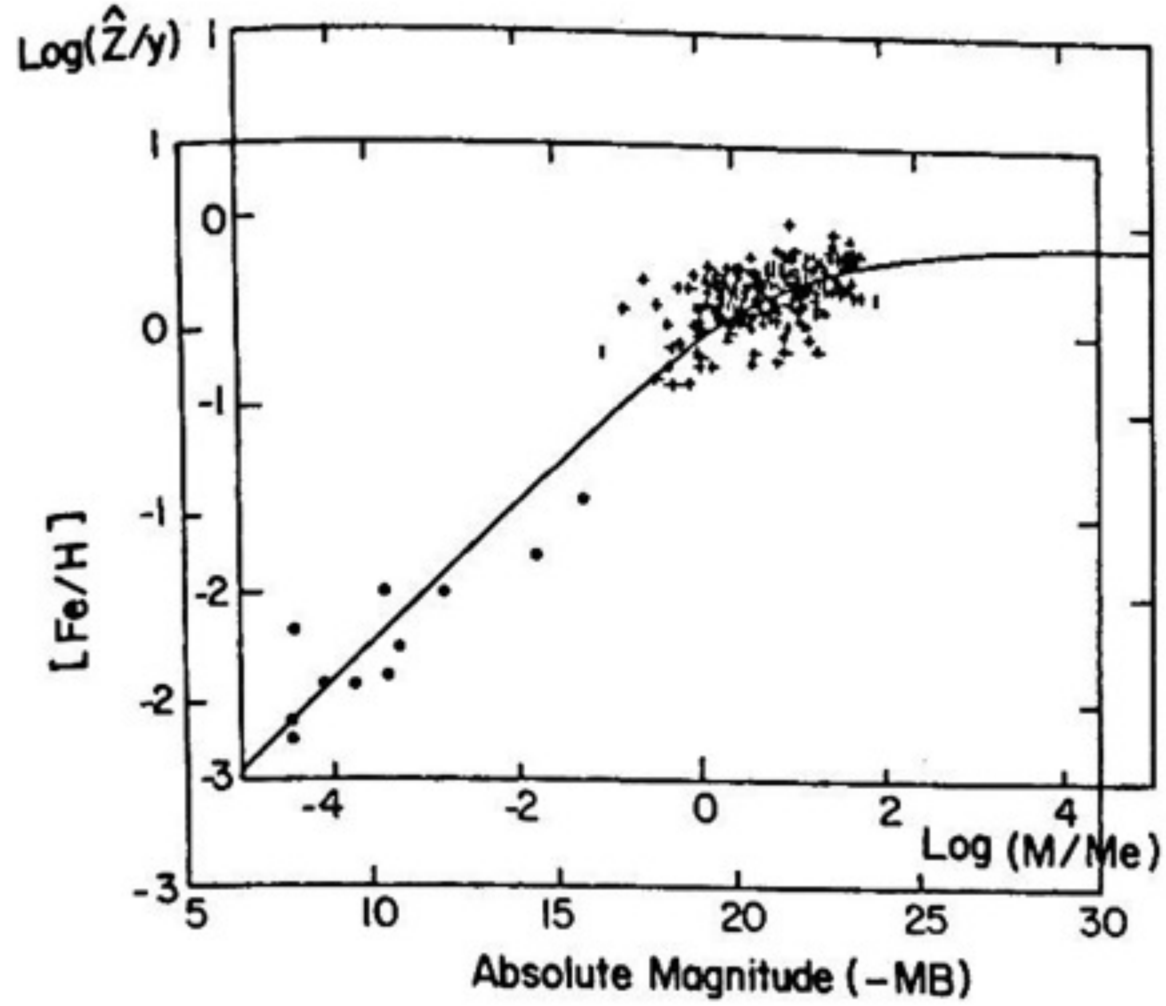

Fig. 11.16. Median metal abundance per unit true yield as a function of final mass with observations of dwarf spheroidal and elliptical galaxies superposed. The offsets of axes determine the characteristic mass M_e that constrains supernova debris and the true yield y (p in the text). MB is the corresponding blue absolute magnitude (neglecting any dark halos). The trend along the linear branch of the curve is for metallicity to increase approximately as $M^{1/2}$. After Lynden-Bell (1992).

“Merger models”

- Bursts intensos de formação estelar estão associados a mergers de sistemas ricos em gás (galáxias luminosas no IV).
- Há varios argumentos de que elípticas massivas se formaram dessa forma (Toomre 77; Kormendy & Sanders 92; Barnes 95), provavelmente seguido a mergers de halo de matéria escura
- a colisão de grandes nuvem de gás leva a:
  - formação estelar
  - dissipação de energia
  - eventual expulsão de gás por SN
- primeiros modelos químicos de Tinsley & Larson (1979)

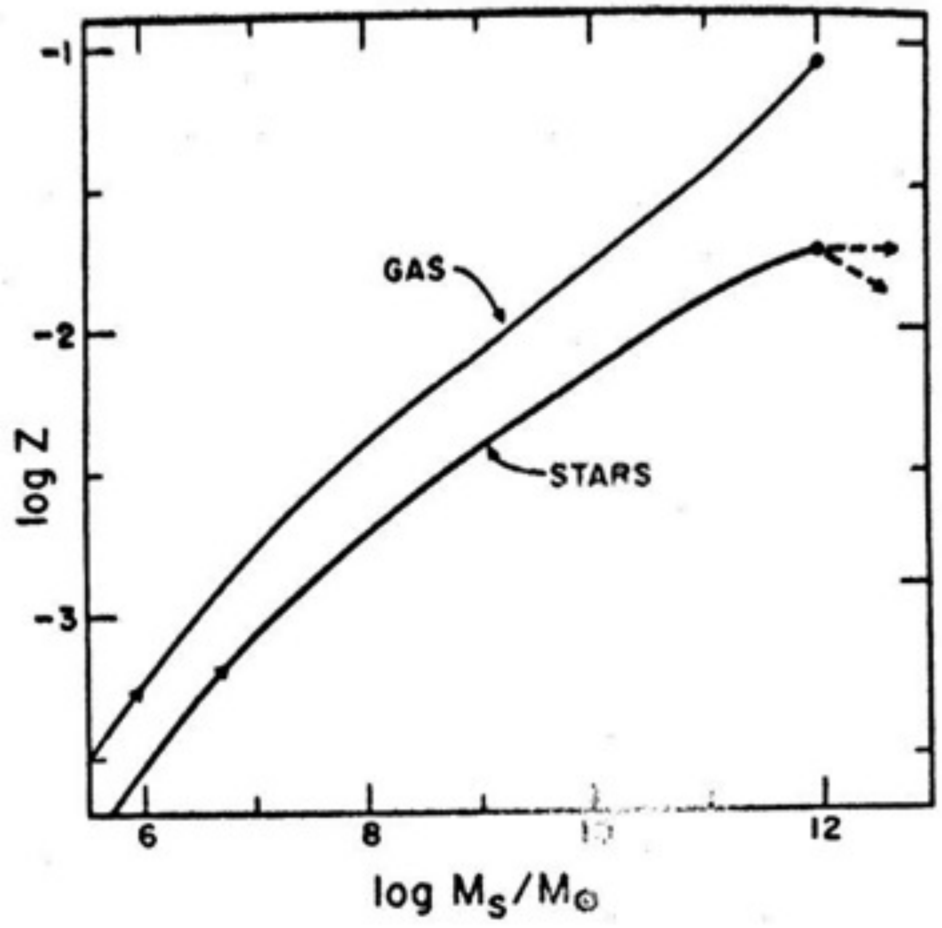

Fig. 11.17. Metallicities of stars and gas as a function of the total mass of stars in an elliptical galaxy growing by mergers, assuming a true yield of 0.02. The trend is for stellar Z to increase approximately as $M^{1/2}$ for small masses, flattening to $M^{1/4}$ for larger ones. Filled circles show the point beyond which there will be little star formation in mergers because the gas cannot cool sufficiently between collisions; arrows indicate possible outcomes of further mergers without star formation. After Tinsley and Larson (1979).

Merger models

Formação de elípticas por mergers

- Dois cenários foram modelados por Thomas, Greggio & Bender (1999)
    - "Fast clumpy collapse": galáxias massivas são formadas por mergers de curtas escalas de tempo (~1Gyr). A taxa de formação estelar é relativamente constante durante o merger. Dissipação causa gás enriquecido a cair para o centro do sistema. O resultado não é muito diferente do modelo de colapso monolítico de Larson (1974). [α/Fe] aumenta com a distância ao centro.
    - "Merging spirals": O merging ocorre em sistemas que já converteram a maior parte de seu gás em estrelas. Durante o merging, o gás enriquecido residual cai para o centro e um episódio intenso de formação estelar ocorre. Leva a valores mais baixos de [α/Fe] do que o cenário de cima. [α/Fe] é mais alto no centro da galáxia resultante.
    - A existência do fundamental plane indica o primeiro cenário. O segundo cenário é visto atualmente em Ultra-luminous Infrared Galaxies.